ABSTRACT

RAJAGOPALAN, AJIT. Antenna Design for Ultra Wide Band Communications and Frequency Selective Surfaces. (Under the direction of Professor Gianluca Lazzi).

In narrow band systems, the use of multiple antennas at the transmitter and the receiver, implementing what is traditionally known as Multiple Input Multiple Output (MIMO) system, has been shown to provide increased channel capacity as compared to a single antenna system. Whereas traditional MIMO systems employ arrays of antennas that are separated by half a wavelength, MIMO systems implemented using orthogonal co-located loops and dipoles have been shown to be able to deliver the same capacity of traditional systems. In 2002, the Federal Communications Commission (FCC) approved the use of ultra wide band (UWB) devices operating in the frequency range 3.1 - 10.6 GHz. Since then efforts have been made to design ultra wide band systems for communications purposes. Ultra wide band systems promise increased data rates over short distances compared to traditional narrow band systems. Such systems can find applications in home networks, corporate wireless networks and also military communications. Since MIMO systems employing co-located antennas in the narrow band case deliver increased channel capacity as compared to a single antenna system, the design of co-located antenna systems for ultra wide band communication can potentially provide similar increases in capacity over a wide band.

The current work reports the design of such a vector antenna for an ultra wide band communications system. The vector antenna system consists of a loop antenna and two orthogonal bowtie antennas. It is shown that these antennas have a broad bandwidth, transmit and receive narrow pulses and have low mutual coupling. The performance of the antenna system is evaluated in a rich scattering environment and capacity calculations show that the channel capacity obtained is approximately equal to those employing a linear array of UWB antennas. It is also shown that the co-located vector antenna provides approximately a three fold increase in capacity as compared to a linear array of UWB antennas. An alternate design of a UWB vector antenna which is not co-located but distributed in space is also described. This antenna is smaller compared to the co-located antenna and provides similar increases in capacity.

Vector antennas can not only be used as active arrays but also as individual elements in passive arrays which is also investigated in this work. These arrays produce reflections at certain frequencies and allow transmission at others forming Frequency Selective Surfaces (FSS). Preliminary results including the reflection co-efficient curves for different geometries are reported. A vector antenna design of an FSS is described in detail which resonates at multiple frequencies producing a distinct signature.

Antenna Design for Ultra Wide Band Communications and Frequency Selective Surfaces

by
Ajit Rajagopalan

A dissertation submitted to the Graduate Faculty of
North Carolina State University
in partial fullfillment of the
requirements for the Degree of
Doctor of Philosophy

Electrical Engineering

Raleigh, North Carolina

2008

APPROVED BY:

Dr. Griff Bilbro	Dr. Zhilin Li
Dr.Gianluca Lazzi Chair of Advisory Committee	Dr. Brian L.Hughes

DEDICATION

To my advisor, guru and mentor Dr.Gianluca Lazzi

BIOGRAPHY

Ajit Rajagopalan received the B.E. degree in Electronics and Telecommunications from the University of Mumbai, Mumbai, India, in 2002 and the M.S. degree in Electrical Engineering from North Carolina State University, Raleigh, in 2004, respectively. He continued to work towards the Ph.D. degree in Electrical Engineering at North Carolina State University. Since August 2003, he has been a Graduate Research Assistant with the Department of Electrical and Computer Engineering, North Carolina State University. His research interests include developing novel antenna geometries for ultra wide band (UWB) communications, designing vector antennas and frequency selective surfaces.

ACKNOWLEDGMENTS

First and foremost I would like to thank my parents for encouraging me every step of the way and for their unconditional love and support throughout the Ph.D. program. They took a substantial risk in funding part of my graduate studies and I hope they get handsome returns on their investment. My advisor Dr.Gianluca Lazzi has been an advisor in the very real sense of the word. His valuable insight in problems as well as in depth understanding of the subject were absolutely indispensable in my success and were a source of inspiration. I would also like to thank him for having a patient ear to any questions that I had and for also giving me freedom to try out my own ideas. I would like to thank Dr.Brian Hughes whose inputs on Information Theory were invaluable in the progress of my research and also for being a great teacher of the subject.

Throughout my research career, I've had the opportunity to work with some extraordinary people in different fields all of whom have had a tremendous influence on my success in the program and my career in general. I would like to thank Dr.Keyoor Gosalia for getting me started in the research group and being my initial mentor. His insights into antennas and their working were the initial stepping stone on which I built my research. It was a great pleasure to work with Dr.Anand Konanur who began research on vector antennas and whose ideas were instrumental in removing key roadblocks that I faced from time to time. I also had the pleasure of collaborating with Dr.Gaurav Gupta and this work would not have been completed without him. His grasp of fundamentals was second to none and he is certainly one of the most brilliant people I have ever worked with. Working with Dr.Gupta was an inspired learning experience for me. My work was made easy by standing on the shoulder of these giants. My thanks to Dr.Vinit Singh who was not only a colleague but also a good tennis partner and a very good friend. Discussions with him on any topic have always been very helpful. It was fun to work with Randy Barlow in whose presence there was never a dull moment in the lab and whose humor was always helpful in making a tough day easy. I also enjoyed working and collaborating with other members of the group – Dr.Stefan Schmidt, Patrick Kelly Brown, Shruthi Soora, Carlos Cela, Srinivas Jasti, Sundar Srinivas, Ajeet, Amit Qusba, Zhengxin Tong and Nitin Kwatra. I also had the pleasure of interacting with Dr.Ajith Kamath, the consummate intellectual and erudite scholar with whom discussions on any topic were always enjoyable.

My thanks goes out to my close friends– Salil, Sibin, Meeta, Nikola, Sarat, Surendra, Dhruba and Radha. They were supportive every step of the way and I learnt a lot from their experiences in the pursuit of their graduate degrees. They formed a good support group with whom I could easily share my successes and my frustrations. I would like to thank Glen Garner for giving me the opportunity to serve as the Vice President of Eta Kappa Nu and for being a good friend. My thanks also to Tara Britt whose enthusiasm brought new life to the ECE department and for being very supportive of every single student effort and for doing everything possible to make each student's career a success. I also owe it to her for helping me find my career path. Last but not the least, I would like to thank folks at International Office – Elizabeth Rose Behringer, Kelia Hubbard and Hanya Redwan for making my stay at NC State a breeze by taking care of all immigration related issues promptly and dispensing valuable advice every time.

TABLE OF CONTENTS

LIST OF FIGURES

Chapter 1

Introduction

The origins of ultra-wideband radio can be traced back to the early spark-gap emitters first proposed by Maxwell, and later used by Marconi in his 1901 demonstration of the wireless telegraph. During the 1960's and 1970's impulse radars were investigated first for governmental purposes to obtain greater resolution and larger relative bandwidth. The experiments with radar led to research on impulse radio or broadband radio. In this form of communication, signals are transmitted in the form of very narrow pulses. This is called carrier-less transmission because no sinusoidal carrier is used. These extremely short pulses use a large bandwidth and therefore they are called ultra wide band (UWB)signals.

UWB systems have many potential advantages over conventional narrow band systems in particular applications [2]. In recent years, there has been a growing recognition that UWB offers several unique capabilities that can enable a host of new sensing, positioning, and communication applications. They could potentially be low cost and complexity systems, have a noise like signal of very low power, be resistant to severe jamming and multipath effects and have time domain and tracking applications. Since ultra wide band systems use very narrow pulses they can be separated out at the receiver. This has two benefits: Firstly, multipath components from the same transmitter can be well resolved thereby reducing multipath interference. Secondly, pulses from two different users can also be well separated offering lower inter symbol interference[3],[4]. This offers applications in communications, radar and ranging. The UWB signal has a low spectral density and is noise like. Although there is some ongoing research in this area it seems that this noise like nature of the UWB signal makes it possible for the system to exist with other wireless systems operating in the same frequency band. Since carrier signals are not present, there

is no need for upconversion or downconversion at the transmitter and receiver respectively. Therefore, transmitter and receiver circuits for a single user UWB system are conceptually simpler. However, providing for multiple access and higher data rates increases the complexity of the timing circuitry required which may increase costs. The very low duty cycle of UWB pulses implies that they can potentially be able to provide better timing precision and sub decimeter ranging. With material penetration properties, UWB signals offer applications in short range radar. UWB has long been used in Ground Penetrating Radars, and is now being applied to new imaging devices (e.g. Time Domain's RadarVision) which enable law enforcement, fire and rescue personnel to see through walls and debris during emergencies. These devices can also improve safety in construction by locating steel bars, electrical wiring, and utility pipes hidden inside walls or underground.

1.1 FCC 1^{st} Report and Order

In 2002, the Federal Communications Commission (FCC) approved the use of ultra wide band devices operating in the 3.1 - 10.6 GHz frequency range[5]. This was the largest allocation of bandwidth in history to any terrestrial communications system. In the "First Report and Order", the FCC tried to address many issues pertaining to UWB. The most important issue was the interference UWB provided to other already existing communication systems. There were a number of studies conducted by different parties on interference which are discussed in the FCC report [5]. The FCC also defines precisely what constitutes a UWB signal, regulates power emission limits for such signals and defines frequency ranges for different applications.

Consider a bandlimited signal. Let its upper -10 dB point in the spectrum be given by f_H and its lower -10 dB point be given by f_L. Then the fractional bandwidth of the signal is given by

$$B_f = 2\frac{f_H - f_L}{f_H + f_L} \tag{1.1}$$

A signal is defined as a UWB signal if its fractional bandwidth (as defined above) is greater than 0.2 or if the absolute bandwidth of the signal is 500 MHz or more. The report establishes different technical standards and operating restrictions for UWB devices based on their interference potential.

1.2 UWB and MIMO

In the 1990's the demand for high capacity communications increased many fold. With the increased use of cell phones, the existing technologies were found inadequate to meet the soaring demand. The advanced mobile phone system (AMPS) which used analog technology was replaced by the Digital-AMPS or DAMPS standard (also known as US-136). Qualcomm Inc. came up with the IS-95 standard based on CDMA technology which enabled multiple users to access the same bandwidth without interference. The expansion of the internet led to the demand for internet services on mobile devices. This included data and video services in addition to the already existing voice. As more chunks of the frequency spectrum were assigned to different services, spectrum available for new services became scarce and prohibitively expensive. In order to make use of spectrum more efficiently new technologies needed to be developed.

One of these new technologies that showed a lot of promise was multiple input multiple output (MIMO) systems. Such systems use more than one antenna at the transmitter and the receiver. A schematic diagram of a MIMO systems is shown in Fig.1.1. The 50 Ω refers to the terminations of the antennas. Early studies conducted by Foschini and Gans [6] indicated that capacity increases were possible by using MIMO systems. In a rich scattering environment, Telatar showed that the capacity of system consisting of M transmitter and N receiver antennas is min(M,N) times that of a single transmitter receiver system [7]. Traditionally, MIMO systems consisted of antenna arrays where the individual antennas were placed half a wavelength ($\lambda/2$) apart. However with the demand for higher data rates, on handheld and portable devices, compact MIMO antennas are needed.

Different approaches have been pursued to obtain compact MIMO antennas. One approach includes use of dynamic reconfigurable antennas[8]. Another approach uses co-located "vector antennas". Single and dual-polarized antennas have only two degrees of freedom in polarization. However, since the electromagnetic field consists of six individual components(three electric and three magnetic), potentially useful information is lost. A "vector antenna" can possibly detect each of the six individual components of the signal. A 6-element vector antenna consists of three orthogonal loops (magnetic dipoles) and three orthogonal electric dipoles. These antennas can be distributed in space or co-located. Andrews et al [9] propose a "tripole" antenna that consists of three mutually orthogonal dipoles, and show that this antenna improves on the capacity of scalar and dual-polarized

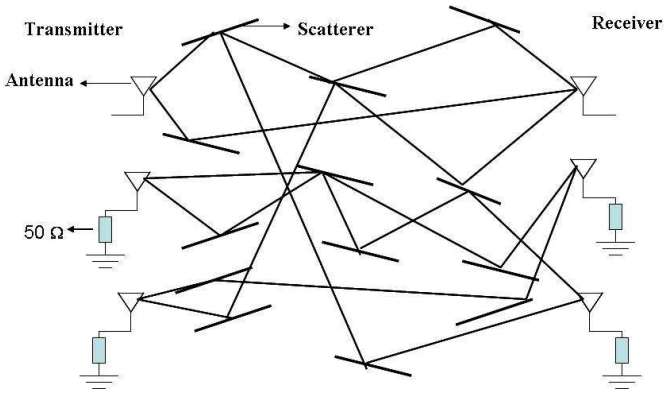

Figure 1.1: Schematic of a multiple input multiple output (MIMO) system

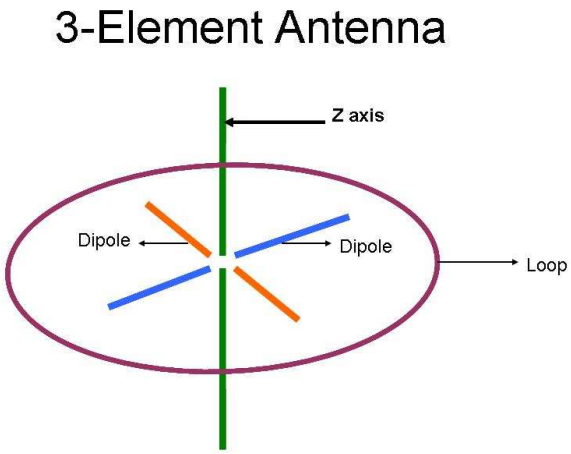

Figure 1.2: Vector antenna consisting of a loop antenna and two orthogonal dipoles

antennas. A co-located narrow band vector antenna consisting of loops and orthogonal dipoles (shown in Fig.1.2) with low coupling, has been shown to provide an increase in capacity as compared to a linear array [10].

Most of the above mentioned work was done with respect to narrow band systems. As seen earlier, UWB systems provide significant advantages like more efficient usage of spectrum, greater resistance to multipath interference and higher range and resolution for detection and tracking applications. However, until 2002 there were no rules or regulations for operating devices that were ultra wide band. The First Report and Order by the FCC in 2002, prompted research into all the different aspects of a UWB system from transmitting and receiving circuits to channel modeling, interference issues and antenna design. Some

antennas were already designed before the FCC "First Report and Order" when antennas were being designed for impulse radiation [11]. Most work on ultra wide band systems has thus far focused on single-polarized electric dipole antennas. Dual-polarized antennas have been extensively studied in certain radar applications, such as ground-penetrating and synthetic-aperture radars. The vector antenna designed in [10] operates over a very narrow bandwidth around 2.2 GHz. Since MIMO systems, with multiple antennas have shown promise in narrow band cases, the application of these concepts to ultra wide band systems could enable the UWB system to access additional degrees of freedom, which could give the same benefits as antenna arrays but by using lesser real estate. They can also find applications in direction-of-arrival (DOA) estimation and medical microwave imaging. The key in such antennas is to make sure that the antennas have very low mutual coupling between them throughout the whole frequency range.

1.3 Applications of Vector Antennas

Vector antennas have a number of applications. Some of the important ones are described briefly below

1.3.1 Wireless Communications

As seen from above, ultra wide band co-located vector antennas are capable of replacing traditional MIMO array antennas. They can provide similar capacities while occupying less space. This is especially an attractive feature for portable devices like laptop computers. The IEEE 802.11n and IEEE 802.15 standards are attempting to include MIMO technology in their framework. Some companies have already introduced MIMO routers in the market. With the development of RF circuitry for UWB communications, MIMO routers using UWB technology should be available in the near future. Vector antennas will provide compact means of designing these routers.

1.3.2 Frequency Selective Surface Array Design

Other than improving channel capacity, vector antennas can also find applications in other areas. One of these areas is that of periodic structures. A periodic structure is an assembly of identical elements arranged in a one or two dimensional array. Each

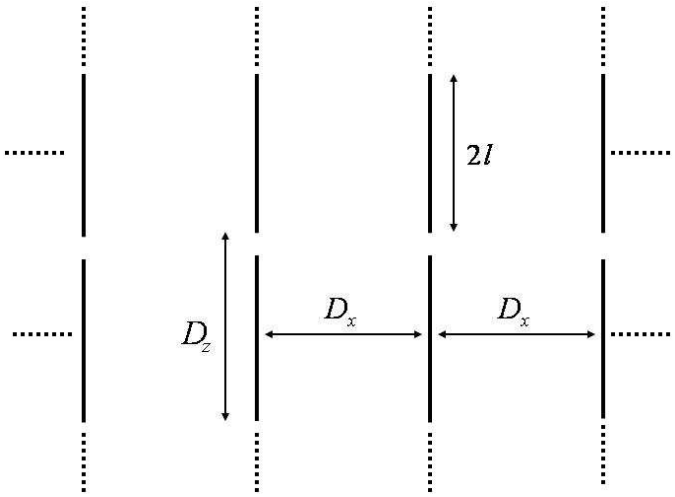

Figure 1.3: Two dimensional infinite array of short circuited dipoles

element represents an antenna like a dipole. An array of antennas can be either active or passive. Antennas can be actively fed by a source connected to each element or they can be passively excited by an incident plane wave. In the latter case the antennas are merely passive structures. In this passive array case, the incident plane wave will be partly transmitted in the forward direction and partly reflected in the backscattered direction. When the array resonates, assuming no grating lobes are present, the amplitude of the reflected signal will be equal to the amplitude of the transmitted signal. This implies that almost all the incident signal is reflected. Since this occurs at a particular frequency, the reflection can be used as a distinct signature. Surfaces which selectively reflect or pass all signals at a particular frequency are called frequency selective surfaces (FSS). They find applications in detection of targets and also making objects transparent to radar. Fig.1.3 shows an infinite two dimensional array of short circuited dipoles which is a simple FSS.

1.3.3 Direction of arrival (DOA) estimation

Radars consisting of narrow band MIMO antennas have been shown to provide better resolution in direction finding applications [12]. Research is also being carried out to use distributed vector antennas (vector antennas spread out in space) to improve DOA estimation [13]. UWB uses very short impulses of the order of nanoseconds with a low duty cycle. Therefore these pulses can provide much better resolution than traditional narrow

band systems. UWB co-located vector antennas show promise in improving resolution, while at the same time providing compactness.

1.3.4 Medical Imaging

UWB vector antennas can also have application in cancer detection and imaging. Early detection and treatment is one of the most important factors in determining the long-term survival of patients with diseases like breast cancer. Microwave imaging techniques have therefore received considerable attention [14]. The use of dual polarized antennas was shown to provide better imaging resolution than unipolarized antennas [15][16]. In UWB imaging the breast is illuminated with a pulse from a conventional UWB antenna, collecting the backscattered signal with the same antenna, and then repeating the process for several different antenna positions. Here again UWB vector antennas promise improvements: They can collect additional components of the backscattered signal and directional data. This can potentially help improve resolution of the image.

1.4 Contribution and overview of dissertation

Considering the encouraging results provided by using MIMO systems in the narrow band case and the FCC's 1^{st} report and order, some very important questions can be asked as follows

- Can the benefits of MIMO systems be extended to UWB frequencies?
- Is it possible to design an ultra wide band vector antenna with low mutual coupling?
- How does such an antenna perform in a rich scattering environment?
- Are there other possible applications for vector antennas?

This work attempts to find answers to these questions and describes the application of vector antennas to frequency selective surfaces (FSS). The design of ultra wide band antennas is different from that of conventional narrow band antennas. Apart from matching the antenna over a wide bandwidth, it is necessary that the radiation pattern of the antennas remain nearly constant with frequency. This means making sure that current distributions in the antennas remain approximately constant. Since the antennas must be able to transmit

and receive very short pulses, they must have a linear phase. Once the individual loop and bowtie antenna is designed, they must be integrated to form a vector antenna with low mutual coupling.

In this work a vector antenna system for UWB communications is designed and investigated. The vector antenna system consists of a loop antenna and two orthogonal bowtie antennas. Chapter 2 describes the design of these antennas and their performance. The elements of the vector antenna operate in the frequency range 3.6 - 8.5 GHz and are fabricated on a single substrate with a relative permittivity of 2.6.

In Chapter 3, the impulse responses of the designed UWB antennas are measured and reported. The antennas are integrated to form a vector antenna with the loop and two orthogonal bowties. Mutual coupling between the antennas is investigated and coupling results for each pair of antennas is reported.

Chapter 4 describes the experimental setup used to evaluate the performance of the antennas in a transmit-receive configuration in a rich scattering environment. The channel matrix is measured and capacity calculations are performed. The capacity obtained is compared to that obtained from a linear array and also to the capacity obtained if only a single antenna at the transmitter and receiver were used.

In Chapter 5, the design of a distributed vector antenna for UWB systems is described. This antenna has lower coupling and also has a better matched loop antenna. The size of the loop antenna is also reduced with respect to that of the c-located vector antenna. In some applications this distributed antenna may be the more optimum solution.

In Chapter 6, frequency selective surfaces are described and results are presented for simple structures. The possible applications of vector antenna to the problem of passive detection is discussed and results are presented for these structures.

Chapter 7 presents conclusions from this work and directions for future research investigations.

Chapter 2

Antenna Design

2.1 Introduction

The object of the current research was to explore whether benefits obtained using narrow band vector antennas could be extended to ultra wide band systems. Since there are six components of the electromagnetic field (three electric and three magnetic), a vector antenna can potentially utilize six elements. The simplest form of vector antenna consists of three electric and three magnetic dipoles. Although this antenna is easy to think of conceptually, in practice it is difficult to construct and will certainly be three dimensional. Most electronic devices today employ printed circuit boards and a three dimensional antenna system would be unwieldy, bulky and difficult to integrate onto printed circuit boards (PCB's). In order to obtain compact antennas that can be easily integrated onto PCB's only planar configurations were investigated. Hence, instead of six antennas, the design of a vector antenna comprising a loop antenna and two dipoles was undertaken.

2.2 Important parameters in the design of UWB antennas

There are some important characteristics that UWB antennas must satisfy. Many of them are similar to narrow band antennas and they will be described in detail in this chapter. Other specifications and performance benchmarks are particular to UWB antennas and these and other parameters particular to vector antennas will be addressed in the next chapter. Some of the common characteristics that define an antenna are [17]

- Return Loss

  The return loss of an antenna is a measure of the impedance mismatch. An antenna has an intrinsic impedance which has a real and an imaginary part. Most radio frequency (RF) systems have characteristic impedances of 50 Ω. Return loss is defined as $20log_{10}\Gamma$. For a characteristic impedance of 50 Ω, Γ is given by

$$\Gamma = (Z_A - 50)/(Z_A + 50) \tag{2.1}$$

  where Z_A is the intrinsic antenna impedance. In order for the antenna to operate in a given frequency range, its return loss must be typically less than -10 dB or less. The lower the return loss, the lesser is the power reflected and greater is the power radiated.

- Radiation Pattern

  The radiation pattern of an antenna is the polar plot of the fields radiated by the antenna in the far field. It gives important information about the components of the fields radiated and also its distribution in space. For a loop in the X - Y plane, the components radiated are E_ϕ and H_θ respectively. For a dipole oriented in the Z direction, they are E_θ and H_ϕ. An antenna should ideally have the same radiation pattern in the frequency band it operates.

- Directivity

  The directivity of an antenna is defined as the ratio of the radiation intensity in a given direction to the radiation intensity averaged over all directions. Directivity is a figure of merit which indicates how well the antenna directs energy in a certain direction. It is given by

$$D(\theta, \phi) = \frac{4\pi U(\theta, \phi)}{P_{rad}} \tag{2.2}$$

  where $U(\theta, \phi)$ is the radiation intensity (power per unit solid angle) of the antenna and P_{rad} is the total power radiated. Radiation patterns in this work will be plotted with their directivity values.

- Gain

  Gain of an antenna is defined as the ratio of the radiation intensity in a given direction to the radiation intensity that would be obtained if the power accepted by the antenna

were radiated isotropically. It is a parameter that takes into account the efficiency of the antenna. Gain is given by

$$G(\theta, \phi) = \frac{4\pi U(\theta, \phi)}{P_{in}} \tag{2.3}$$

where $U(\theta, \phi)$ is the radiation intensity of the antenna and P_{in} is the total power fed to the antenna.

2.3 Loop Antenna

A loop antenna acts as the equivalent of a magnetic dipole. The simplest loop antenna consists of a circular loop fed by a transmission line pair. To behave like a magnetic dipole the loop must have a constant current distribution along its length. This is generally true for loop antennas with circumferences of the order of $\lambda/10$. However, as the circumference of the loop increases beyond this and approaches a wavelength, the current distribution does not remain constant and phase change occurs. The direction of maximum radiation changes from being in the plane of the loop to being along the axis of the loop. It is therefore necessary that the current in the loop is approximately constant at the frequency of operation.

At higher frequencies, the required size of the loop becomes very small. A small loop does not have appreciable radiation resistance. Smith [1] proposed a "cloverleaf" loop antenna for frequency modulation (F.M.) frequencies. This geometry consists of four smaller loops that have a common feed at the center while the other end of each of the four loops is connected to the second conductor of the transmission line. Since each of the individual elements are smaller compared to the wavelength, the current remains constant in them. The currents in adjacent feed lines are directed in opposite directions, thereby ensuring that only circular currents are excited and linear currents are canceled. This reinforces co-polarized radiation and cancels cross polarized radiation and ensures that E_ϕ and H_θ are the dominant radiating components. The geometry proposed by Smith is shown in Fig.2.1.This antenna is also discussed in [18] and briefly in [19]. A cloverleaf antenna using the above principles was designed for a narrowband vector antenna system [10].

There have been several investigations concerning UWB magnetic antennas. A summary of these antennas is reported in [20]. They include large current radiators, scimitar antennas, monoloop antennas and magnetic slot antennas. A compact sectoral loop antenna

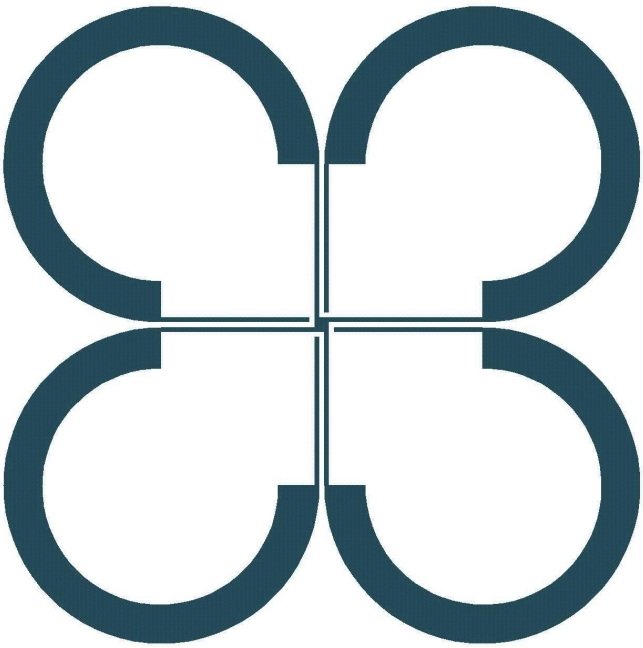

Figure 2.1: Cloverleaf geometry proposed by Smith for F.M.[1]

above a ground plane has also been designed [21]. There have also been efforts to design a broad band loop antenna using multiple loop antennas [22]. However these antennas cannot be integrated into a vector antenna system. Therefore a UWB loop antenna had to be designed that could be incorporated in a vector antenna. For this purpose, the clover leaf antenna of Smith was taken as the starting point and optimized for UWB operation. It is well known that thick loops possess larger bandwidths as compared to thin loops. Therefore the width of the loop was increased and curved in order to obtain a broadband radiating geometry. The radiating element consists of the conducting area between two Quad Folium curves, which are characterized by the polar equation $|r| = 4a \cdot \sin\theta \cdot \cos^2\theta$. A specific design completed in this work utilizes a value of a of 62.5 mm for the outer curve and 43.75 mm for the inner curve. The design was optimized using Agilent Advanced Design System (ADS) to achieve matching over the frequency range from 3.6-8.5 GHz. The geometry of the final loop antenna is shown in Fig.2.2. The four radiating elements were fed at the center by a coaxial connector that maintains constant current and phase in each of the elements. The center conductor of the coaxial connector was connected to the center of the structure and the outer conductor of the connector was soldered through vias to the four ends of the

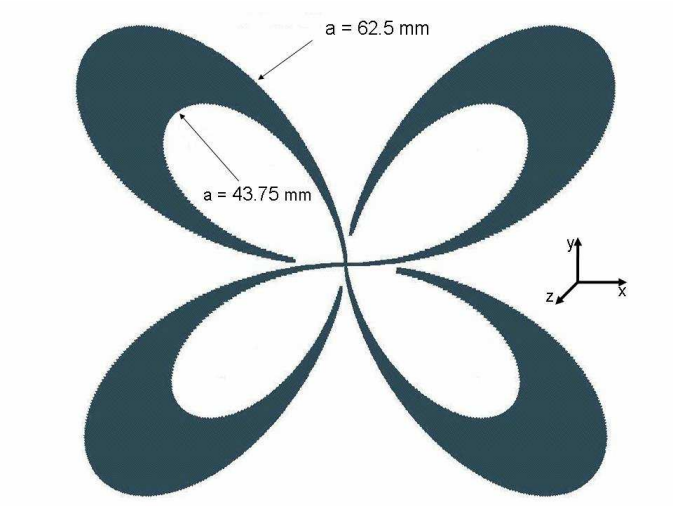

Figure 2.2: Geometry of the UWB loop antenna

radiating elements.

2.3.1 Loop Antenna performance

The performance of the loop antenna will be discussed with respect to return loss and radiation pattern. Fig.2.3 shows the simulated and experimental return loss of the UWB loop antenna. The agreement between experiment and simulation is good, with minor differences that can be attributed to approximations made in the simulations such as the connector not being modeled, and losses in the substrate and conductors not being considered. It can be seen that that the return loss is less than -8 dB (SWR$\leq$ 2.5) over the frequency range 3.6 GHz - 8.5 GHz. The loop antenna is placed in the X-Y plane with the Z axis coming out of the page. The co-ordinate system for the antennas is shown in Fig.2.4.

Radiation patterns obtained from ADS simulations in the X-Z plane at 4 GHz, 6 GHz and 8 GHz, shown in Fig.2.3.1, indicate that the E_ϕ component is the dominant radiating component at all frequencies as expected in a magnetic dipole. The magnitude of the directivity in dBi is indicated in the radiation patterns and this will be indicated in all radiation patterns henceforth. The nulls observed at $\theta = \pm 90^o$ are due to the fact that the simulation is carried out by ADS assuming an infinite substrate in the plane of the loop.

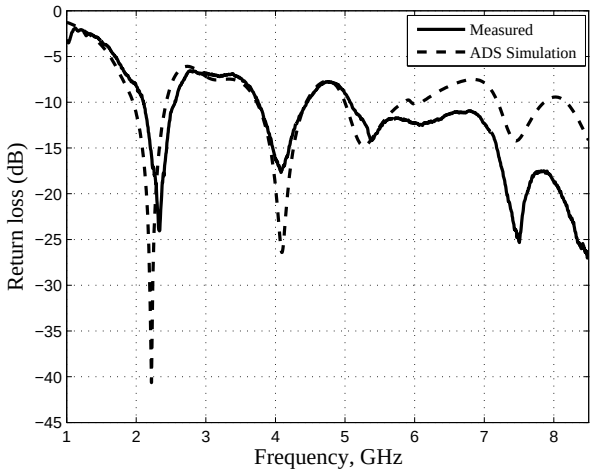

Figure 2.3: Simulated and measured return loss of the UWB loop antenna

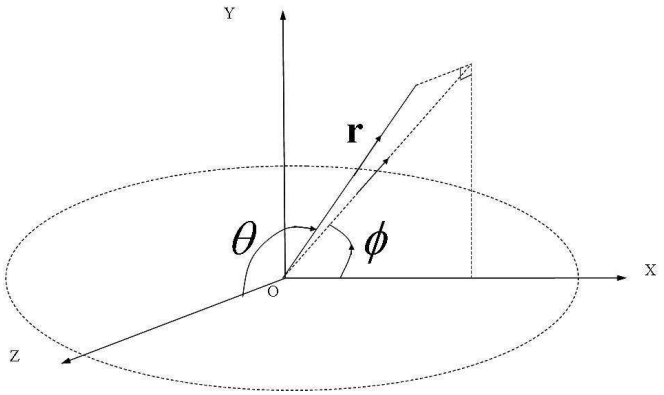

Figure 2.4: Co-ordinate system used to measure radiation patterns

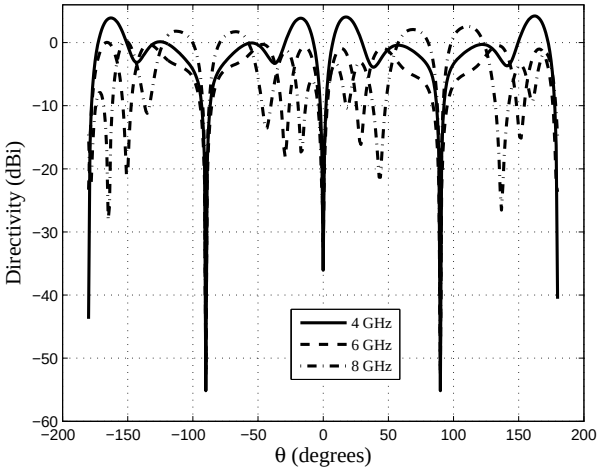

(a)

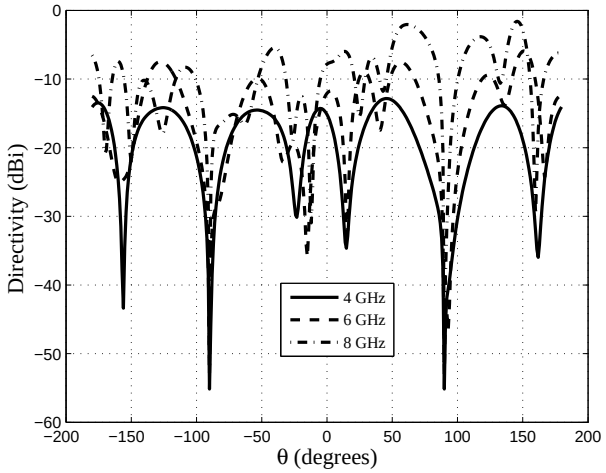

(b)

Figure 2.5: Simulated radiation pattern of the loop antenna in the X-Z plane (a) E_ϕ (b) E_θ

2.4 Bowtie Antenna

Ultra wide band antennas were already being designed prior to the release of the FCC Order primarily for impulse radar applications [23], [11]. After the release of the FCC 1^{st} Report and Order, there was a new impetus directed at the design of ultra wide band dipole antennas. Many different geometries were proposed. Schantz proposed elliptical dipoles and ovoidal dipoles [24] while differential ended elliptical antennas were described in [25]. Another variation was the diamond and rounded diamond antenna [26]. A bowtie monopole with coplanar strip line feed is described in [27].

Wire dipoles are sensitive to frequency. Their current distribution is cosinusoidal only when the wires are infinitely thin. Therefore their impedance as well as radiation pattern change with frequency. This is more pronounced in the cases in which the length of the dipole is such that there is a near null in the current distribution at its input terminals. For the UWB case, impedance and radiation pattern have to be constant over a wide bandwidth. A simple geometry used to obtain broad band characteristics is the biconical antenna [17]. It is formed by placing two cones of infinite extent together at the feed point. The two cones can be thought of as the conductors of a uniformly tapered transmission line. The geometry of a biconical antenna is shown in Fig.2.6 and a detailed discussion can be found in [17]. The characteristic impedance of this line also represents the input impedance of an infinite antenna. The half angle of the cone is chosen so that the input impedance of the antenna is the same as the characteristic impedance of the transmission line feeding it. Computed values of input resistance and reactance are given in [28] and it has been observed that as the cone angle increases, the variations in antenna impedance are less severe and the antenna is more broadband.

The biconical antenna is solid and large in size and therefore impractical for many applications except for VHF and UHF frequency ranges. It has also been used for UWB channel characterization [29]. Because of its promising characteristics, two dimensional approximations of the biconical antenna in the form of the triangular sheet and the bowtie antenna have been investigated. The triangular sheet, which is essentially a monopole version of the bowtie antenna as well as the bowtie antenna have been experimentally investigated in detail, by Brown and Woodward [30]. It was found that a triangular sheet with a larger included angle provided less variation in impedance and radiation pattern with respect to frequency. However, this performance was still inferior to that of a conical

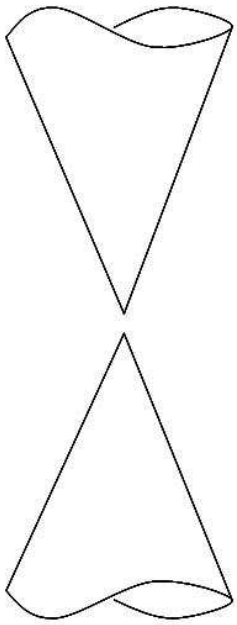

Figure 2.6: Geometry of a biconical antenna

antenna.

Planar dipoles for UWB applications have been proposed in [31] and a bowtie antenna optimized for pulse radiation is described in [32]. The bowtie antenna used for the vector antenna is based on the design proposed by Kiminami et al [33]. He proposed a two sided antenna using a microstrip line feeding section. The antenna has very good impedance matching characteristics, stability of radiation pattern and linear phase. It is compact and can be easily integrated onto a printed circuit board. The antenna has also been used in an array by Eldek et al.[34]. A similar bowtie antenna was designed for the current vector antenna without the microstrip line section in [33]. This made the antenna more compact and enabled easy integration in the vector antenna. The performance of the antenna was not affected by this. The antenna has been fed by a balanced parallel transmission line structure. Once again, the bowtie antennas were optimized using Agilent ADS and fabricated on the same dielectric substrate as the loop ($\epsilon_r = 2.6$). The geometry of the bowtie antenna designed in this work and its dimensions are shown in Fig.2.7. They are W1 = 5.8 mm, W2 = 5.4 mm, W3 = 2.9 mm, W4 = 7.8 mm, W5 = 18.55 mm, W6 = 12.9 mm, L1 = 7.1 mm, L2 = 18.3 mm, L3 = 5 mm, L4 = 14 mm, L5 = 12 mm, L6 = 26 mm.

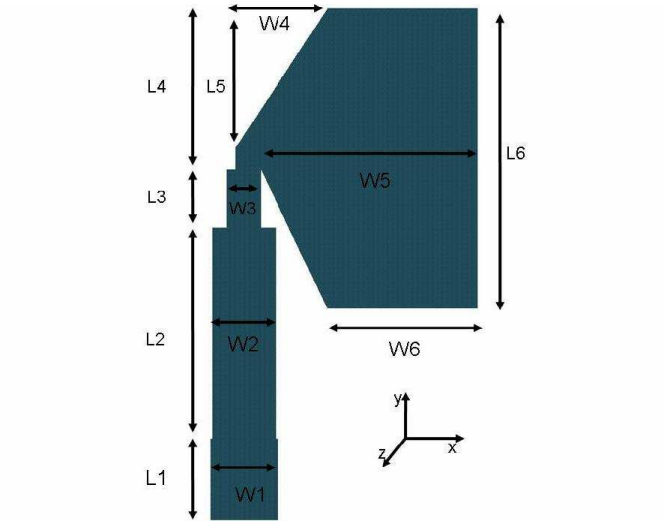

Figure 2.7: Geometry and dimensions of the bowtie antenna

2.4.1 Bowtie Antenna performance

Fig.2.8 shows the return loss of the simulated and fabricated bowtie antenna. Once again, the agreement between experiment and simulation is generally good, with differences below -10 dB that can be attributed in the simplified model used for ADS simulations. The bowtie antenna shows a return loss lower than -10 dB from 3.6 - 8.5 GHz. The bowtie is placed in the X-Y plane and its two arms are along the X-axis. As expected, its simulated patterns in the X-Z plane at the frequencies of 4, 6 and 8 GHz (Fig.2.9) show that the E_θ component is the dominant radiating component at all frequencies.

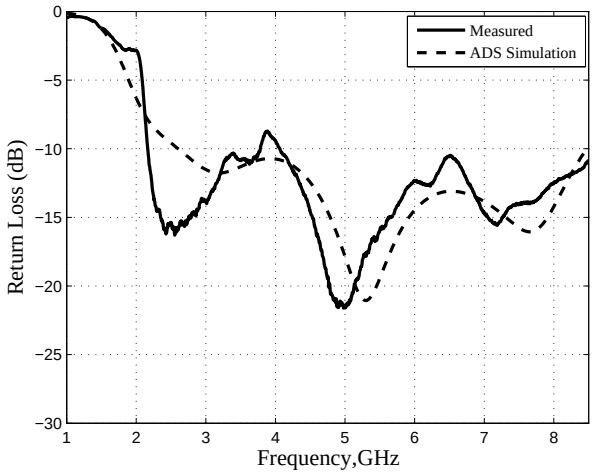

Figure 2.8: Simulated and experimental return loss of the bowtie antenna

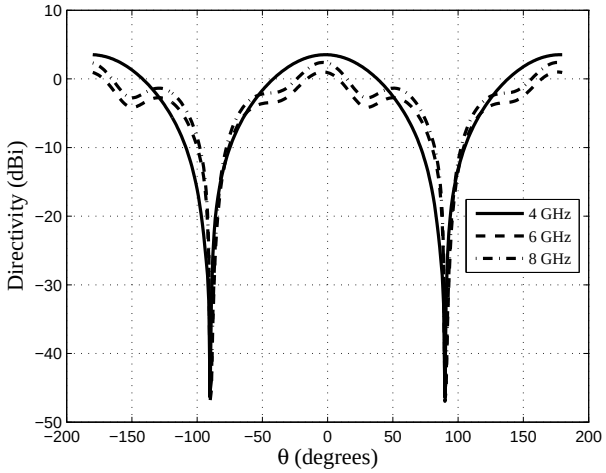

(a)

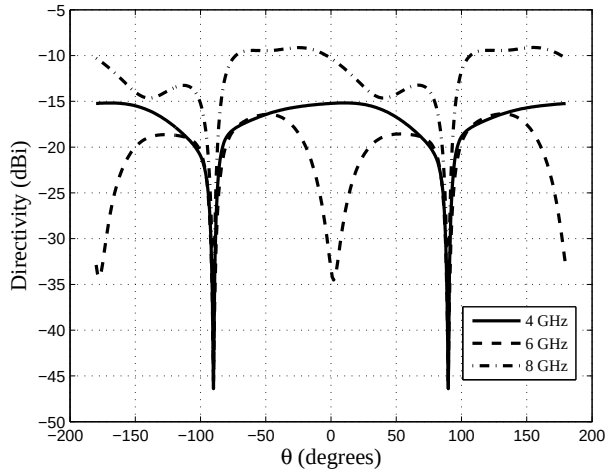

(b)

Figure 2.9: Simulated radiation pattern of the bowtie antenna in the X-Z plane (a) E_θ (b) E_ϕ

Chapter 3

Impulse Radiation and Antenna Integration

3.1 Introduction

As indicated before, ultra wide band systems can transmit and receive very narrow pulses. This presents some interesting challenges in the design of antennas for UWB applications. The antennas used in a UWB system must be capable of transmitting and receiving these pulses without distortion. This chapter will describe the characterization of the UWB antennas in the time domain to verify their pulse transmission and reception fidelity. In order to design a vector antenna, the loop and bowtie antennas were integrated on the same substrate. When antennas are in close proximity of each other, the fields radiated by one antenna induces currents in the other antenna causing loss in radiated energy. This is referred to as mutual coupling. Though some research indicates that mutual coupling could help in de-correlating multipaths [35], the vector antenna was designed with the aim of minimizing mutual coupling. When the antennas are integrated, individual properties such as impedance match and radiation pattern are susceptible to change. It is shown in this chapter that the changes in the antenna properties are small enough to have no significant effect.

3.2 Impulse Radiation

3.2.1 Dispersion

Conventional systems are narrow band and typically operate around a center frequency. These systems are analyzed using frequency domain techniques. Since a very narrow band is considered, a sine or a cosine signal remains essentially unchanged in shape at different points in the communication system. However, this is not the case if broadband pulses are used with antennas. An ideal antenna acts as a differentiator and produces a field which has the same waveform as the second derivative of the input voltage. In other words, an antenna acts as a high pass filter. Therefore some of the lower frequency components are not transmitted leading to pulse distortion. Classical frequency independent antennas use the geometry of the structure to attain a wide bandwidth. These antennas are based on the principle that the performance of the antenna remains unchanged if its electrical length remains the same [17]. The geometry of such antennas is typically specified in terms of angles only. Spiral antennas and log periodic antennas fall into this category. The small scale portion of the antenna radiates at higher frequencies and the large scale portion of the antenna radiates at lower frequencies. Therefore, there is a change in the phase center of the antenna with frequency and at any point in the far field there exists a delay in signals arriving from different points of the antenna leading to dispersion in the received pulse. This is seen in a response that has ringing and is stretched out in time. The phenomenon also varies according to the look angle of the antenna i.e. a different response will be obtained for each look angle. For UWB applications, pulses need to be reproduced faithfully. This means that the phase center of the antenna must remain stationary.

3.2.2 Time Domain Response

An antenna can be tested using different methods for its time domain properties. A typical experimental arrangement consists of two antennas that are aligned in the direction of maximum radiation. One method is the direct time domain method. In this method, one of the antennas is connected to an impulse generator. An impulse generator usually generates pulses by differentiating step functions. The generator is adjusted to produce a pulse that occupies the required bandwidth. The other antenna is connected to a sampling oscilloscope. The receiving oscilloscope must be triggered at the right time to record the

pulse.

The second method uses frequency domain techniques. In this method the two antennas are connected to the two ports of a vector network analyzer (VNA). The VNA is used in the time domain mode of operation. In this mode the VNA calculates the frequency response and uses the inverse Fourier transform to estimate the impulse response. In the present case, the frequency domain method is used. The VNA was adjusted to give a transmitting pulse of width 0.218 nS, where the pulse width is measured at 50% of the maximum amplitude. The measurements were conducted in an indoor environment to simulate real world conditions.

Measurement

The loop antennas were placed side by side so that they are aligned in the direction of their maximum radiation. The maximum dimension of the loop antenna across the diagonal is 20 cm. Considering the highest frequency of 8.5 GHz, the far field distance is approximately $2D^2/\lambda = 2.26$ m. The loop antennas were placed at a distance of 2.3 m. The bowtie antennas were placed facing each other at a distance of 15 cm which corresponded to the far field distance for these antennas.The time domain impulse response S_{21} of the antennas is shown in Fig.3.1.

It can be seen from Fig.3.2.2 that the loop antenna receives a narrow pulse of width 0.232 ns and the bowtie antenna receives a pulse of width 0.291 ns. Therefore although there is some broadening of pulses at the receiving antenna, the pulses are still sub nanosecond. This indicates that the antennas can transmit and receive narrow pulses used in UWB communications. There are some trailing components in each case. These are likely due to antenna ringing or reflected components. For additional confirmation of pulse transmissions, the phase of the impulse response is measured. If the impulse response has linear phase then we can conclude that the main pulse is faithfully reproduced and the components arriving later are reflected components of the signal from the surrounding environment. The phase responses of the loop and the bowtie antennas are shown in Fig.3.2.

From the phase responses we see that the bowtie antenna has almost perfectly linear phase while the loop antenna has approximately a linear phase. Therefore we can say that the additional components in the impulse response of the bowtie are only due to reflections. The loop does have some non linearities in phase and this shows as ringing in

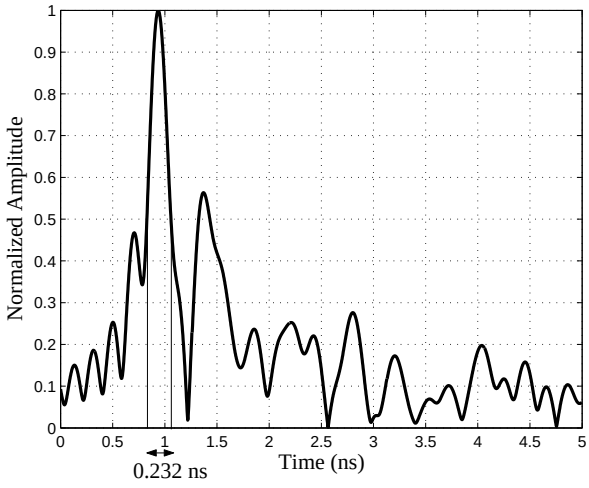

(a)

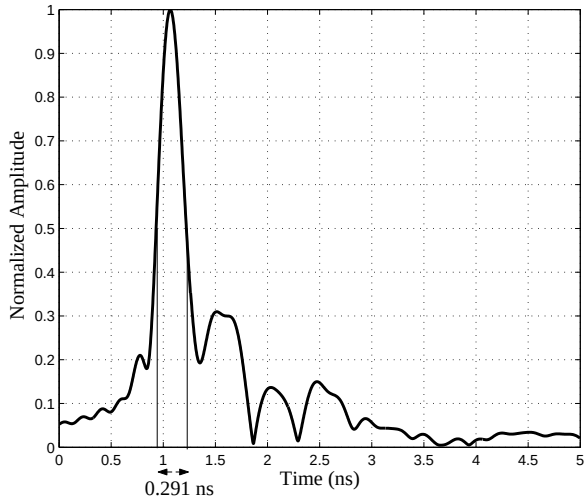

(b)

Figure 3.1: Impulse responses of the loop and bowtie antennas (a) Loop (b) Bowtie

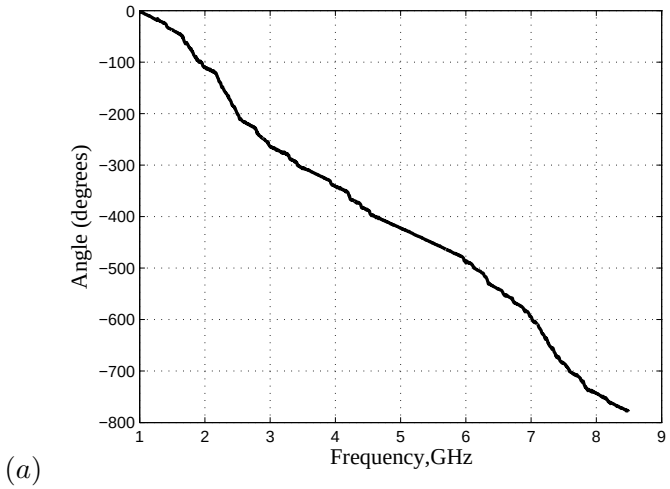

(a)

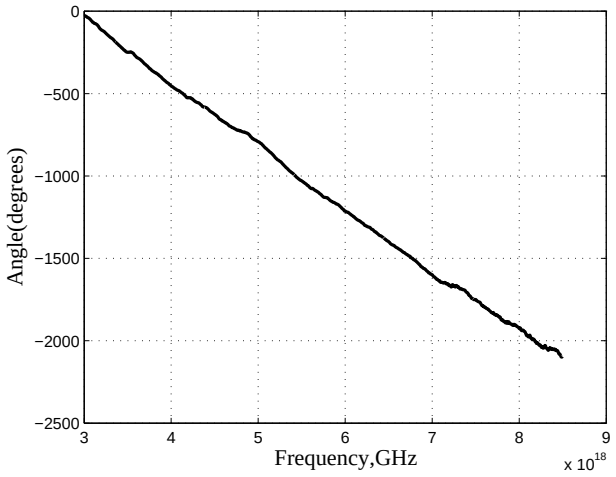

(b)

Figure 3.2: Phase responses of the loop and bowtie antennas (a) Loop (b) Bowtie

the impulse response. However, it is not at a detrimental level.

3.3 Vector Antenna Design

The simplest six element vector antenna configuration consists of three dipoles and three loops. However, since the focus of the current research was on planar structures, a system consisting of a loop and two dipoles was constructed. The loop antenna was integrated with the two bowtie antennas to form a co-located vector antenna system. The bowtie antennas were placed in the plane of the loop and approximately orthogonal to each

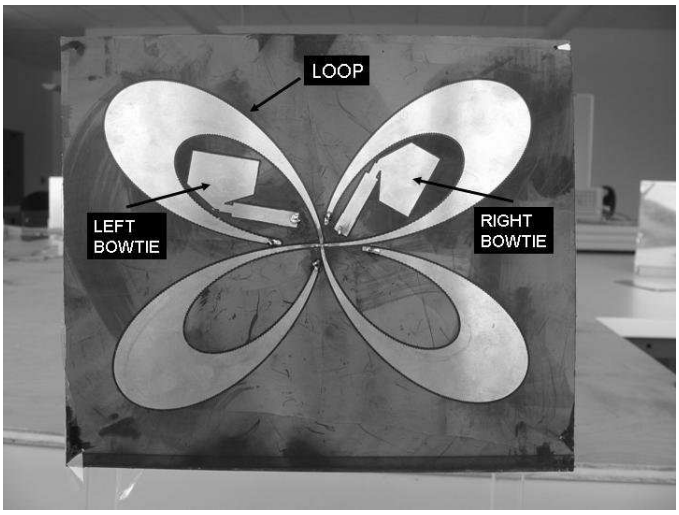

Figure 3.3: Vector Antenna

other to obtain maximum isolation. This was done to ensure that polarization diversity between the orthogonal bowties as well as the pattern diversity between the loop and the bowtie could be exploited fully. The feed points of the left and the right bowties were at co-ordinates (-9.1 mm, 9.6 mm) and at (7 mm, 4.8 mm) respectively with respect to the feed point of the loop (0 mm, 0 mm). Fig.3.3 shows the fabricated Vector Antenna [36].

3.3.1 Mutual Coupling

Traditionally multiple input multiple output (MIMO) antennas are placed in an array, typically half a wavelength apart. In such cases the effect of one antenna on the other antenna was negligible. However, when antennas are co-located as described above, it gives rise to the problem of mutual coupling. Mutual coupling occurs because fields radiated by one antenna induce currents in a neighboring antenna due of their proximity. It is defined as the ratio of voltage produced at the terminals of one antenna element to the voltage excitation at the input terminals of another antenna with all the remaining antennas terminated in matched loads. Coupling can reduce the radiation efficiency [37]. The coupling between antenna elements was measured by connecting the two antennas under test to the two ports of an Agilent E5071-B Network Analyzer and terminating the third antenna in a matched load of 50 Ω. The coupling results for the UWB vector antenna system is shown in Fig.3.4.

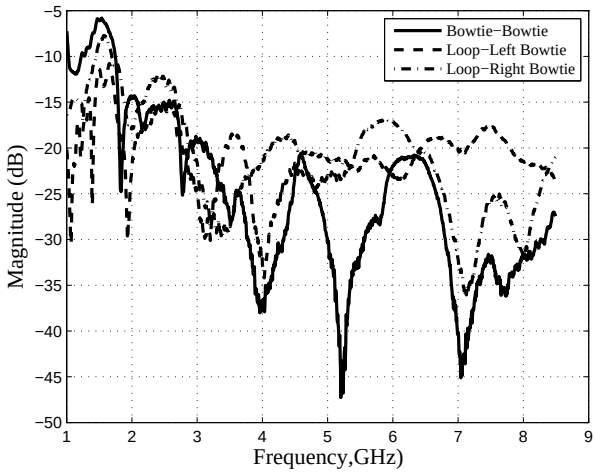

Figure 3.4: Mutual Coupling between individual antenna elements of the Vector Antenna

From the figure we can see that mutual coupling is less than -15 dB over the frequency band of interest (3.6 GHz - 8.5 GHz) for all possible combinations of antennas. This indicates very good isolation and implies that less than 4% of the power is coupled between the antenna elements. The coupling between the bowties is even lower ($\leq$-20 dB) indicating very high isolation. Therefore the information transmitted individually by the antennas will be independent of each other and this could increase the number of degrees of freedom available leading to an increase in capacity.

3.3.2 Impedance Mismatches and Radiation Pattern

Close proximity of the antennas and mutual coupling can also affect the impedance matching of the antennas. The antennas which were well matched individually, could potentially display some mismatches after integration. In order to measure this, the return loss for each of the individual antennas was measured with the other antennas terminated in a matched load. The results are shown Fig.3.5. From the figure it can be seen that the bowtie antennas continue to be well matched. There is some deterioration in the return loss of the loop antenna, particularly in the frequency range 6.72 GHz - 7.11 GHz, although this not at a level to be detrimental for channel capacity.

Radiation pattern of the antennas can also undergo distortion. The radiation patterns of the individual antenna elements need not be the same that were observed with

(a)

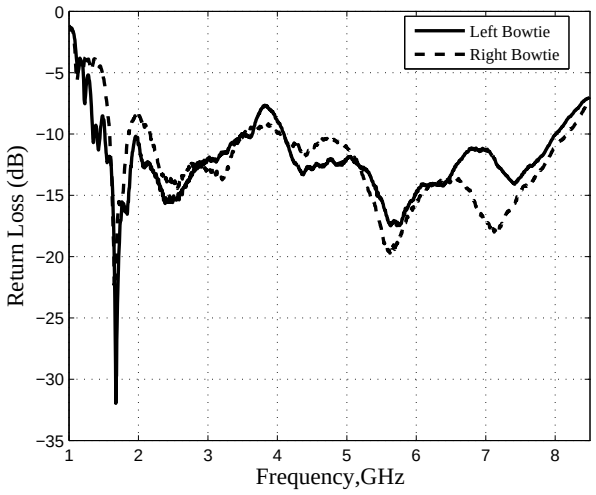

(b)

Figure 3.5: Return losses after integration for the loop and bowtie antennas (a) Loop (b) Bowties

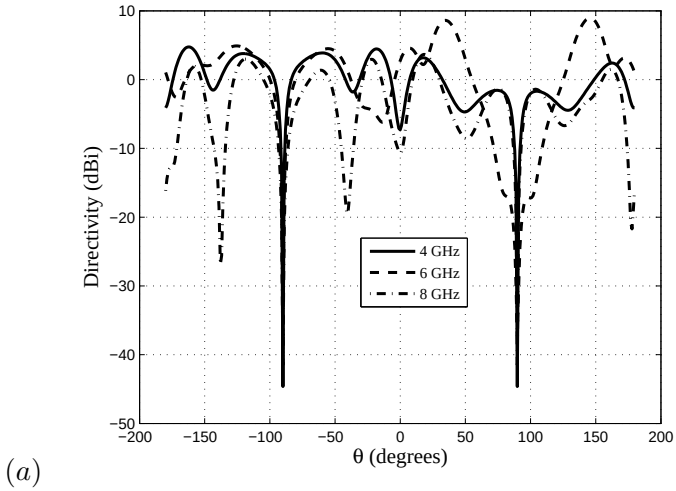

(a)

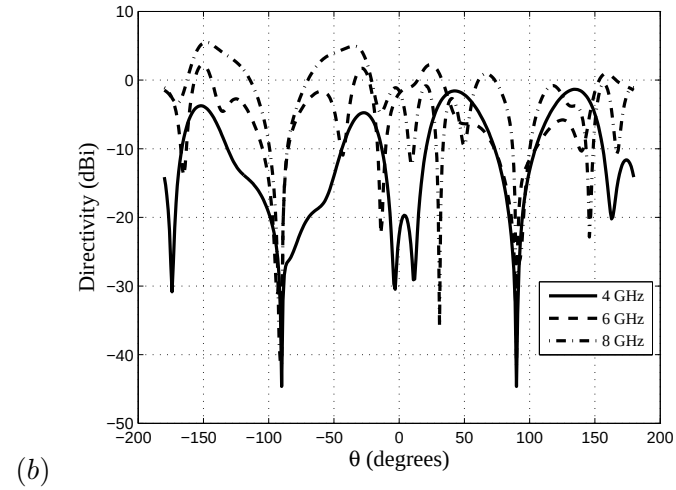

(b)

Figure 3.6: Radiation pattern of the loop antenna after integration (a) E_ϕ (b) E_θ

the antennas in isolation. This is particularly true about cross polarization components. The loop antenna primarily radiates the E_ϕ component while the E_θ component constitutes cross polarization. For the bowtie, E_θ is the main radiated component. Radiation pattern purity was determined by simulating each antenna individually and terminating the others in matched loads. The results for the loop antenna are shown in Fig.3.6 and for the bowtie in Fig.3.7.

From the figures it can be seen that there is some deterioration with respect to the cross polarized component for the loop as well as the bowtie. This effect is particularly pronounced at higher frequencies. However, the main radiating component for the loop

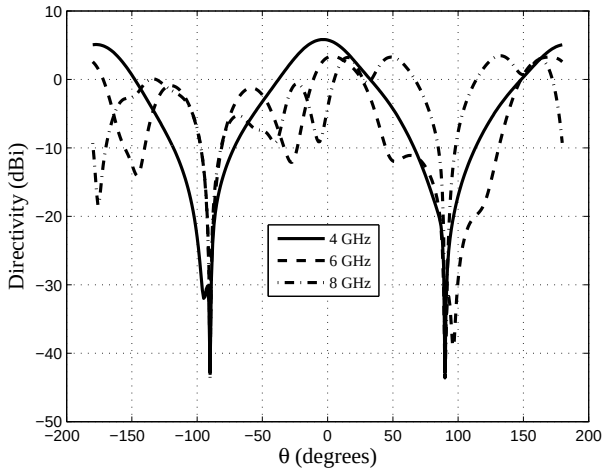

(a)

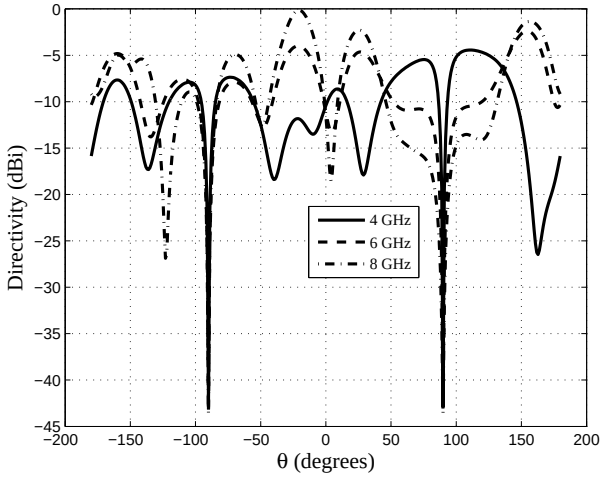

(b)

Figure 3.7: Radiation pattern of the bowtie antenna after integration (a) E_θ (b) E_ϕ

still remains E_ϕ and that for the bowtie remains E_θ. This confirms that the loop is still radiating as a magnetic dipole and the bowtie as an electric dipole.

Chapter 4

Channel Measurement and Capacity Calculations

4.1 Introduction

The characteristics of the vector antenna designed up to this point have been verified according to the parameters required of ultra wide band antennas. The usefulness of the antennas can only be verified when these antennas are used in a real transmitter-receiver setting and channel capacity is calculated. Channel conditions may change on a continuous basis. Therefore, it is necessary to calculate the capacity of the channel under different channel realizations and verify whether the results are consistent across these channel realizations. This chapter describes the use of vector antennas in a realistic environment. The experimental setup and the measurement procedure are described in detail. The method used for calculating capacity is described and results are plotted for the capacity of a vector antenna compared to that of a linear array as well as for the capacity of the three antenna system compared to that of a single antenna at the transmitter and the receiver.

4.2 Channel Measurement Methods and Issues

An ultra wide band channel has an extremely rich multipath profile. UWB signals have an extremely large bandwidth, hence the corresponding time resolution of the channel is of the sub nanosecond order. Similar to measuring the impulse response, there are time

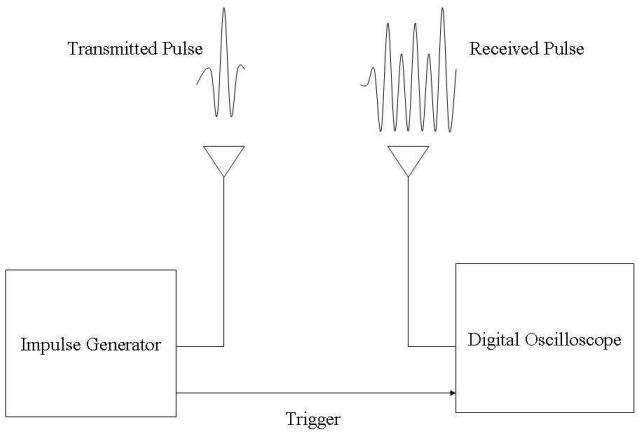

Figure 4.1: Schematic for time domain sounding

domain and frequency domain techniques to measure the UWB channel impulse response which constitute entries in the channel matrix. [38].

- Time Domain : The UWB channel matrix can be determined completely in the time domain by measuring the impulse response of the channel. However, it is not possible to measure the true impulse response, because of the unavailability of the ideal Dirac delta function. Instead, the channel can be measured in the time domain using channel sounders which essentially produce impulses of very short duration. The generator is connected to the transmitting antenna and an oscilloscope to the receiving antenna. A train of narrow pulses is sent from the transmitter separated by sufficiently long idle periods so that all the multipath components can be collected at the receiver. The response observed on the oscilloscope constitutes the impulse response of the channel. This method is also useful to measure time varying channels. The bandwidth of the pulse can be controlled by varying its width. However, this method has some disadvantages. It is difficult to obtain an impulse generator that allows us to control the transmitted pulse with precision. The receiving oscilloscope also needs a triggering mechanism to account for the finite time of propagation of the pulse from the transmitter to the receiver. A simple schematic of this system is shown in Fig.4.1 [38]. Time domain sounding can be also be carried out by using Direct Sequence Spread Spectrum (DSSS) sounding which is discussed in detail in [39].

- Frequency Domain : The frequency domain technique is based on the measurement of the channel at discrete frequency points using a frequency sweep by a vector network analyzer (VNA). The main advantage of using this technique is the larger dynamic range leading to improved measurement precision. There is no need for a triggering signal in this case because both the transmitter and receiver are synchronized internally. Each measurement is represented by a complex number containing the magnitude and phase of the channel gain. The two ports of the network analyzer are connected to the transmitting and receiving antennas respectively. The network analyzer performs a frequency sweep sending narrow band sinusoids at each frequency point within the frequency interval. The number of frequency points is dictated by the resolution which can be set by specifying the lower and upper edges of the frequency band of interest. However, there are some limitations with this method as well [40]. The most important limitation is that the channel should remain constant over the duration of the frequency sweep. The maximum sweep time should be less than the channel coherence time, otherwise, the channel may change during the sweep. Another factor to be taken into account is the maximum channel delay. The upper bound for the detectable delay τ_{max} is given by [40]

$$\tau_{max} = \frac{N_{smp} - 1}{B} \tag{4.1}$$

where N_{smp} is the number of frequency points and B is the bandwidth selected. The length of the cables could also be a factor in the measurement. The longer the cable, the greater is the time of travel for the sounding signal. The receiver needs to be synchronized with the transmitter while the frequency sweep occurs. If this is not the case, the receiver might sample the channel at a higher frequency than intended, leading to errors in the estimation of the channel [41]. The error in frequency is given by [40]

$$\Delta f = \ t_p(\frac{B}{t_{sw}}) \tag{4.2}$$

where t_p is the time of propagation and t_{sw} is the sweep time. This can be overcome by using frequency stepping instead of frequency sweeps. In frequency stepping the VNA steps between frequency discretely with finite time intervals between each step. If the time interval between the steps is greater than the propagation time, the response for a given input signal will be obtained before the VNA steps to the next higher

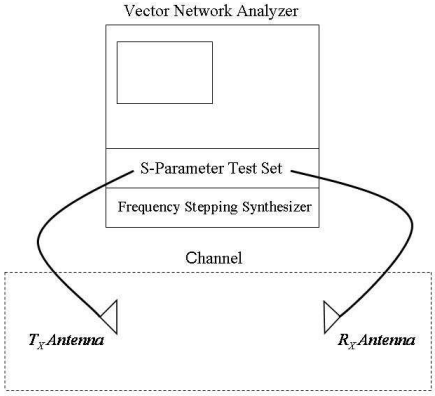

Figure 4.2: Schematic for frequency domain measurement

frequency, thus ensuring accuracy in measurement. If the frequency error is less than the IF bandwidth of the VNA, reliable measurements are obtained. A frequency domain channel measurement system similar to the one described above is discussed in [42] and a measurement system using a sophisticated triggering system is described in [43]. A simple schematic of the frequency domain setup using just one transmitting and one receiving antenna is shown in Fig.4.2 [41].

4.3 Channel Measurement

4.3.1 Setup

In this work, we have used the frequency domain technique to measure the channel coefficients. Two prototypes of the vector antenna were constructed and used in a transmitter receiver configuration. Since six antennas are used (three at the transmitter and three at the receiver) and the channel response is required for each pair of antennas, a port extender in the form of a switching matrix was used in conjunction with the network analyzer to enable seamless transition between antenna pairs fairly quickly. This reduced the probability of experiencing channel variations during measurement. The switching matrix was an Agilent 87130A switch driver with option K01. This switch driver had the capability of extending ports to a 6×6 system. At any instant of time, only two of the switches

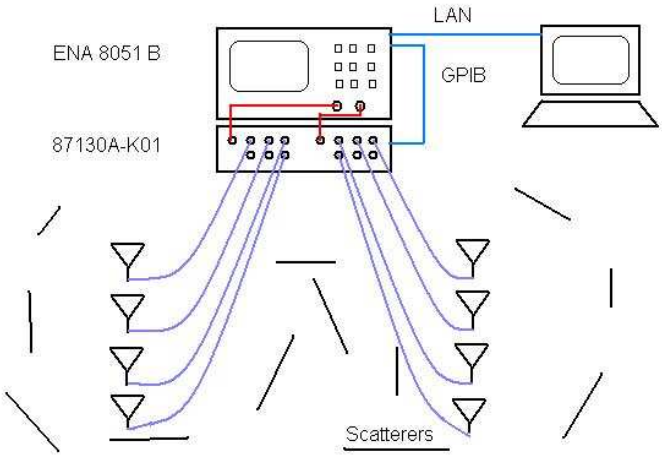

Figure 4.3: Schematic of measurement test bed

were closed (one each at the transmitter and receiver) connecting a pair of antennas to the VNA while all the inactive switches were terminated in matched loads of 50Ω. The switch driver was connected to the network analyzer through a USB/GPIB interface and the network analyzer itself was connected to a PC through LAN connection.The instruments were controlled from the PC through GPIB commands sent via a VISA interface [44].

The transmitting and receiving antennas were separated by distance of 4.5 m which is twice the far field distance of the loop antenna. The environment consisted of metal scatterers (acting as perfect reflectors) placed randomly in the far field of the antennas along the whole range in a laboratory setting to simulate a rich scattering environment. There were 23 metal scatterers of different sizes. The direct path between transmitter and receiver was blocked to simulate a non line of sight (NLOS) channel. This was the case for all channel measurements. The schematic of the measurement test bed is shown in Fig.4.3 and is the same as used in [44].

4.3.2 Measurement

Consider $i-th$ receiver as port 2, the $j-th$ transmitter as port 1 as shown in Fig.4.4. Let V_1 and V_2 be the total voltages at ports 1 and 2 respectively.

$$h_{ij} = \frac{V_2}{V_1} = \frac{V_2^+ + V_2^-}{V_1^+ + V_1^-} \tag{4.3}$$

where the '+'and '-'superscripts indicate incident and reflected voltage waves re-

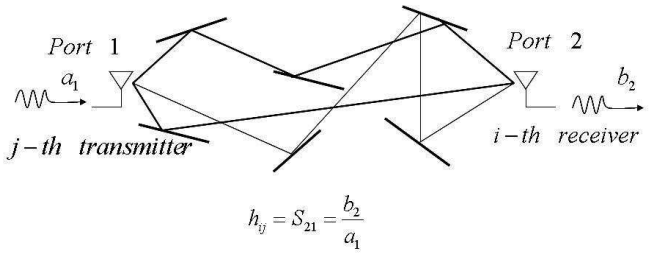

Figure 4.4: Measurement of channel matrix using S-parameters

spectively.

Let

$$a_1 = \frac{V_1^+}{\sqrt{Z_{01}}}, a_2 = \frac{V_2^+}{\sqrt{Z_{02}}}, b_1 = \frac{V_1^-}{\sqrt{Z_{01}}}, b_2 = \frac{V_2^-}{\sqrt{Z_{02}}} \tag{4.4}$$

where Z_{01} and Z_{02} are characteristic impedances of ports 1 and 2 respectively.

$$h_{ij} = \frac{(a_2 + b_2)\sqrt{Z_{02}}}{(a_1 + b_1)\sqrt{Z_{01}}} \tag{4.5}$$

Since the antennas are matched to $Z_{01} = Z_{02} = 50\ \Omega$ we can consider the traveling voltage waves to be essentially the total voltages at the respective ports. i.e. $a_2 = 0$ and $b_1 = 0$. Therefore we have

$$h_{ij} = \frac{b_2}{a_1} = S_{21} \tag{4.6}$$

The the $i, j-th$ entry of the channel transfer matrix H is found by measuring the transfer S-parameter S_{21} using a Vector Network Analyzer (VNA) while the other antennas are terminated in 50 Ω loads.

The VNA was set to operate on a frequency range from 1 GHz - 8.5 GHz. This range was divided into 1601 equally spaced points. Therefore the frequency resolution is given by

$$\Delta F = \frac{7.5 \times 10^9}{1601 - 1} = 4.6875 MHz \tag{4.7}$$

The maximum detectable delay is

$$\tau_{max} = \frac{1}{\Delta F} = 213.3 nS \tag{4.8}$$

The maximum distance for transmission measurement is given by

$$L_{span} = \frac{c}{\Delta F} = 64m \tag{4.9}$$

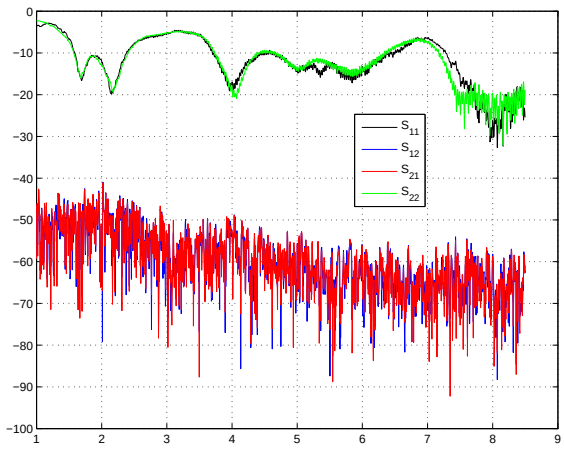

Figure 4.5: Measured channel parameters for the case of loop antennas at the transmitter and receiver

Since the distance between the antennas is only 4.5 m, the setup is well within the limit. The temporal resolution is $1/\Delta F = 133.33$ pS. The intermediate frequency bandwidth of the VNA was set to 500 Hz. This automatically set a sweep time of 3.3 s. The frequency error that may occur due to long propagation delay is given by

$$\Delta f = t_p(\frac{B}{t_{sw}}) = 34Hz \tag{4.10}$$

This is less than the IF bandwidth of 500 Hz. A set of 40 channel measurements were taken by changing the scattering environment for each measurement. The scatterers were randomly distributed on the test bed. Once the scatterers were placed, the surrounding environment was unchanged. Fig.4.5 shows a sample measurement for a loop antenna at the transmitter and a loop at the receiver. S_{11} and S_{22} represent the return losses of the loop at the transmitter and receiver respectively and S_{21} and S_{12} represent the channel transfer function.

4.4 Capacity Calculations

A measure of the utility of the antennas in this application is the ergodic capacity [7] of the resulting communication channel. Consider the following system model for the received signal

$$\mathbf{y} = \mathbf{Hx} + \mathbf{n} \tag{4.11}$$

where $\mathbf{H}$ is the channel transfer matrix, $\mathbf{x}$ is the transmitted signal and $\mathbf{n}$ is the noise vector with independent and identically distributed (iid) components $\sim N(0,1)$. We assume that the Channel State Information (CSI) is known only at the receiver. The UWB channel is divided into $N = 1046$ sub-bands of bandwidth $\Delta f = (W_1 - W_0)/N$ where $W_0 = 3.6$ GHz is the lower end of the spectrum and $W_1 = 8.5$ GHz is the upper end. Assuming that the channel is approximately constant over the Δf bandwidth centered at frequency f_n, the capacity of this t $\times$ t narrowband system at signal-to-noise ratio (SNR), P is given by

$$C(f_n) = \log_2 \left| \mathbf{I} + \frac{P}{t(W_1 - W_0)} \hat{\mathbf{H}}(f_n) \hat{\mathbf{H}}(f_n)^\dagger \right| \quad \text{bits/s/Hz} \tag{4.12}$$

Note that the channel matrices in the above capacity calculation have been normalized according to

$$\hat{\mathbf{H}}(f_n) = \mathbf{H}(f_n)/\alpha \tag{4.13}$$

where

$$\alpha = \sqrt{\frac{\sum_{i=1}^{t} \sum_{j=1}^{t} \sum_{n=1}^{N} |H_{ij}(f_n)|^2}{t^2 N}} \tag{4.14}$$

to remove the effect of path loss. For the case of uniform power distribution over the frequency band, the capacity of the UWB system can be calculated using the following formula [45], [46]

$$C_{UWB} \approx \frac{1}{N} \sum_{n=1}^{N} C(f_n) \quad \text{bits/s/Hz} \tag{4.15}$$

For UWB systems, the FCC has allowed a maximum emission of -41.3 dBm/MHz in the 3.1-10.6 GHz frequency range. Thus, considering thermal noise at 300K, the maximum value of signal power per unit bandwidth to noise power per unit bandwidth $\rho = P/(W_1 - W_0)$ is 72 dB. The expected value of the capacity is calculated by averaging the capacity over all channel realizations. Fig.4.6 compares the expected value of the capacity of the vector antenna system calculated from channel measurements to the capacity of a simulated 3 $\times$ 3 system with iid complex gaussian entries and no coupling between the antennas (which corresponds to the case of spatially well separated antennas). It can be noted that the capacity of vector antenna system is approximately equal to that of the traditional spatial array and at high SNR's their slopes are almost the same. Since at high SNR's the slope of the curve is proportional to the rank of H, we can conclude that 3 degrees of freedom exist.

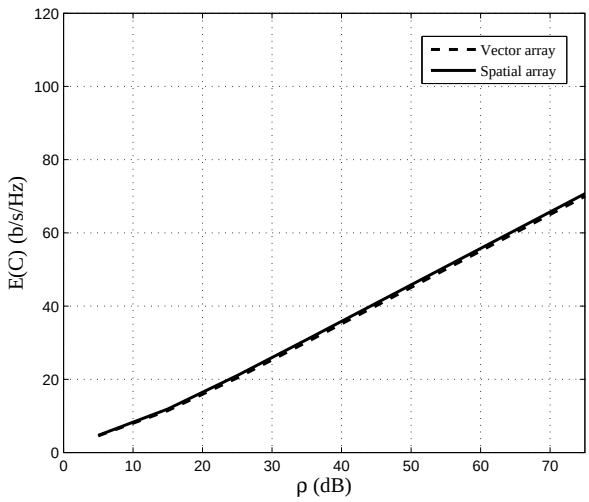

Figure 4.6: Expected value of the Capacity of the Vector Antenna compared to that of a traditional Spatial Array

A measure of performance gain by using polarized antennas is the ratio of capacity using tri-polarized antennas to the capacity using just uni-polarized antennas. As there could be three possible directions for uni-polarized antennas we take the average of capacity for each polarization. Therefore, the gain is given by

$$G = \frac{E(C_v)}{\frac{1}{3}\sum\limits_{i=lb,rb,loop} E(C_i)} \tag{4.16}$$

where $i = v, lb, rb, loop$ for the vector, left bowtie, right bowtie and loop antennas respectively. Fig.4.7 shows the gain v/s ρ. It can be observed that there is approximately a three fold increase in capacity of the vector antenna system as compared to the system using bowtie or loop antennas only.

It has been shown that a vector antenna system can provide almost the same capacity as a linear array. It is therefore a compact solution to the multi antenna problem. Since, we find almost a three fold increase of the capcity as compared to using a single antenna system the vector antenna provides additional degrees of freedom. It must also be noted that the above results were calculated for a uniform input distribution. The input distribution can be further optimized by using the water filling algorithm in which more power will be sent through the channel that has lesser noise and vice versa. This can be implemented if knowledge of the channel is fed back to the transmitter [7]. The uniform

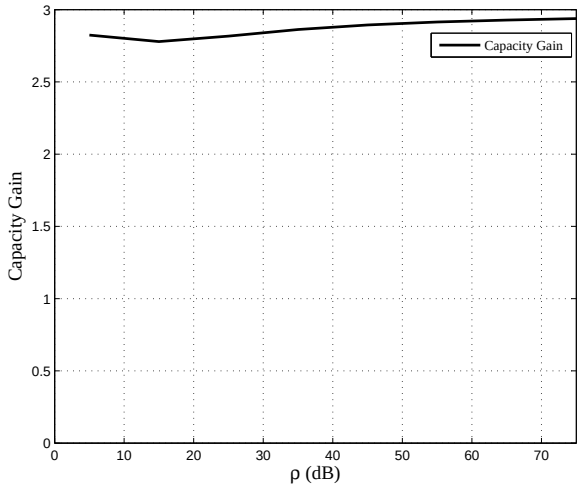

Figure 4.7: Capacity gain of the 3 element Vector Antenna compared to a single antenna system

power input distribution is thus the worst case capacity and hence provides a lower bound.

Chapter 5

Distributed Vector Antennas

5.1 Introduction

Although co-located vector antennas are compact, sometimes the coupling between them may not be acceptable. It might also lead to an unwieldy construction because of the feeds being very close to each other. One solution to this problem is provided distributed vector antennas. A distributed vector antenna consists of closely spaced antenna elements distributed in space [13]. The feeds of the antennas are separated from each other and therefore this antenna system resembles a traditional array. The main difference is that the array elements are different and spacing between them may be small. These distributed vector antennas can be arranged linearly or circularly. A narrow band distributed vector antenna is shown in Fig.5.1. The antenna is designed to operate at 3 GHz . This antenna was used in direction of arrival estimation applications [13]. Since narrow band distributed vector antennas have shown improved results in direction of arrival (DOA) applications, this idea can also be extended to broad band and ultra wide band antennas. In previous chapters, we have discussed a co-located ultra wide band vector antenna; this chapter will discuss a distributed ultra wide band vector antenna design.

5.2 Antenna System

The distributed vector antenna system consists of a clover leaf loop and two orthogonal bowties as shown in Fig.5.2 . As described earlier, the clover leaf loop has some mismatch problems in the presence of the bowtie antennas. This problem can be alleviated

Figure 5.1: Fabricated narrow band distributed vector antenna consisting of a loop and two dipoles

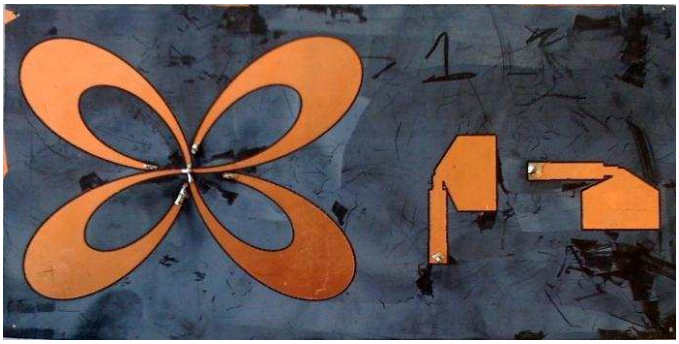

Figure 5.2: Fabricated distributed vector antenna consisting of a clover leaf loop and orthogonal bowties

by spacing the antennas. The antenna elements in this case can also be optimized individually to meet the UWB specifications. The loop antenna was optimized to obtain the best impedance match in the frequency range 3 - 8.5 GHz. The equation of the curves used to describe the loop is same as described in Chapter 2 (in the equation $|r| = 4a \cdot \sin\theta \cdot \cos^2\theta$, a for the outer curves is 45 mm and that for the inner curves is 31.25 mm). The antenna was fed as described in Chapter 2. The simulated and measured return loss for the loop antenna is shown in Fig.5.3. It can be seen that the matching obtained is better than that in Fig.2.3.

The bowtie antennas are perfectly orthogonal to each other. The distance between

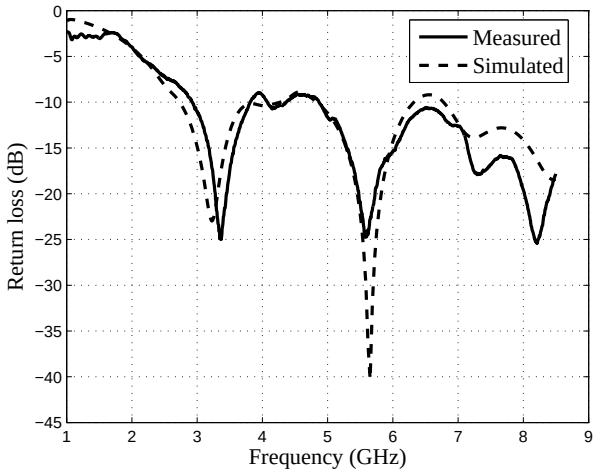

Figure 5.3: Simulated and measured return loss of reduced size loop antenna

the loop and the vertical bowtie is 8.8 cm (which is 0.88λ at 3 GHz) and the distance between the bowties is 6.4 cm (0.64λ at 3 GHz). Therefore the antenna separation in each case is more than half a wavelength. The coupling between the individual antennas is shown in Fig.5.4. The antennas operate in the 3 - 8.5 GHz range and have very low coupling($\leq$ -20 dB) between them providing excellent isolation. This particular antenna system has an area of 209.25 cm^2 as compared to 252 cm^2 of the co-located vector antenna. This antenna system therefore presents a reduction in area of 42.75 cm^2 achieved mainly because of the decrease in the size of the loop antenna.

5.3 Capacity Calculations

The distributed vector antenna system was also used in a transmitter receiver configuration. The channel was simulated using randomly placed scatterers and capacity calculations were carried out for 40 such realizations. The capacity obtained by using this antenna system was almost the same obtained from that of a linear array as shown in Fig.5.5. The capacity was also found to be almost 3 times the capacity of a system using one transmitting and one receiving antenna as shown in Fig.5.6. Therefore the distributed vector antenna is a more compact realization of the vector antenna with the same performance as the former. It can therefore be concluded that in the case of ultra wide band systems a distributed antenna system might be more useful than a co-located system. This primarily

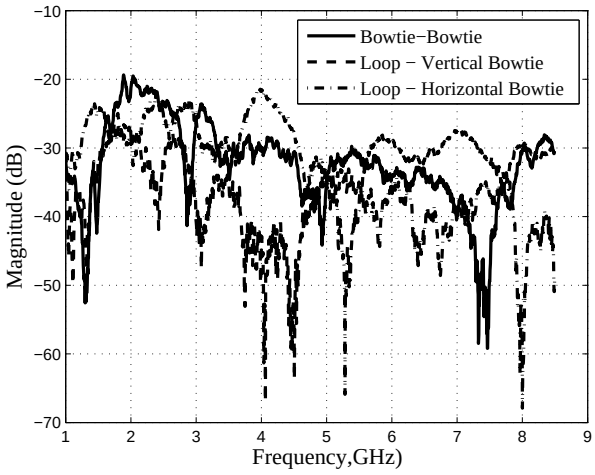

Figure 5.4: Coupling between individual antenna elements of the distributed vector antenna

occurs because UWB antennas do not consist of merely thin wires as in the case of narrow band antennas.

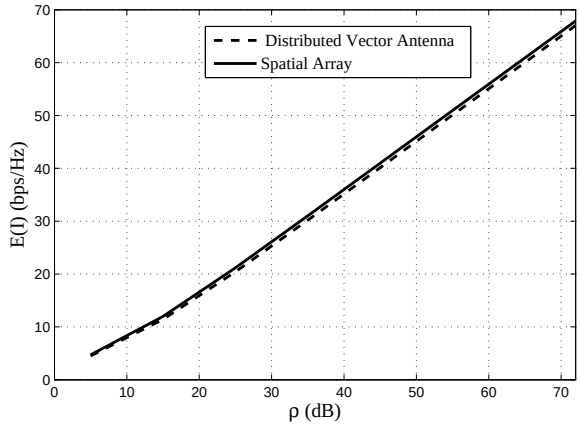

Figure 5.5: Expected value of the Capacity of the distributed Vector Antenna compared to that of a traditional Spatial Array

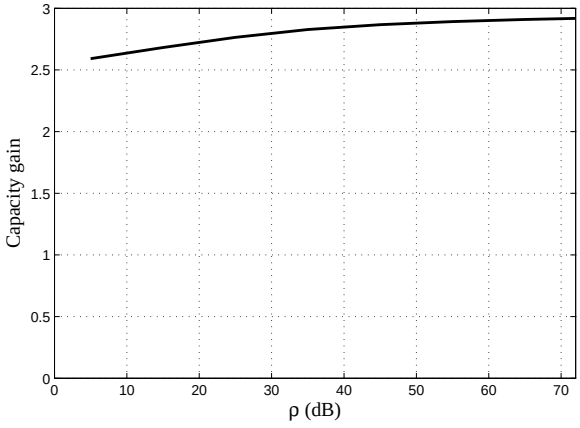

Figure 5.6: Capacity gain of the 3 element distributed Vector Antenna compared to a single antenna system

Chapter 6

Frequency Selective Surfaces

6.1 Introduction

Frequency Selective Surfaces (FSS's) were first investigated in the 1970's when the design of radomes for antennas was researched. A radome is a structural, weatherproof enclosure to protect an antenna. A radome should provide protection to the antenna while not interfering with the normal functioning of the antenna. Therefore radomes need to allow signals in the operating frequency range of the antenna to pass through while keeping out other signals. Thus a radome is a frequency selective surface (FSS). In reflecting back out of band signals an FSS can produce a weak reflected signal in the backscatter direction while producing a strong reflection in other directions. This reduces the Radar Cross Section (RCS) of antennas and is particularly useful for antennas mounted on military aircraft. Examples of FSS's include arrays of dipoles, slots, loops and other geometries. Each of these designs has some advantages and disadvantages.

The idea behind the current research was to develop a class of resonating arrays that will respond with a distinct backscattered signature when illuminated by microwave radiation. The objective of this study is to demonstrate through simulation that it is indeed possible to produce distinguishing signatures using an antenna array. To this end, simple geometries were simulated in order to develop a thorough understanding of the characteristics of the reflected fields. Once the simpler geometries were characterized, vector antennas were used. It will be shown that these vector antennas produced multiply resonating surfaces that can produce a unique signature.

6.2 FSS Design Issues

There are several important considerations in the design of an FSS. The most important are the resonant frequency, excitation of grating lobes, bandwidth, and stability of the reflection co-efficient with respect to angle of incidence and polarization. Although, a complete quantitative description of performance can only be obtained through simulation, there are several guidelines as well as rules of thumb that can aid in a good starting design, which can then be optimized through computer simulation. For example, consider a two dimensional array of short circuited dipoles shown in Fig.6.1. The arrangement of these dipoles in the array is of critical importance. If the dipoles are placed further away from each other (typically greater than half a wavelength apart), the reflection co-efficient varies considerably with angle of incidence. There is also the problem of grating lobes or side lobes in which part of the reflected energy is used up. This means that lesser energy will be reflected in the direction of the main beam. If the antennas are brought close together, grating lobes are eliminated and the variation of the reflection co-efficient with angle of incidence is also minimized. However, the structure now becomes broadband [47]. To obtain a distinguishing signature, the spacing between the elements needs to be adjusted so that the no grating lobes occur and at the same time the surface is relatively narrow band. Vector antennas can be used to obtain signatures with different polarizations and provide additional degrees of freedom.

6.3 Loops and Dipoles

The common geometries used traditionally for designing FSS's can be classified into four groups [48]. They are

1. Center Connected N poles
2. Loop geometries
3. Solid Interior plate types
4. Combinations of earlier groups

Most details of these geometries as well as reflection co-efficient curves are given in [48]. It is shown that the four legged loaded loop element has the most attractive properties

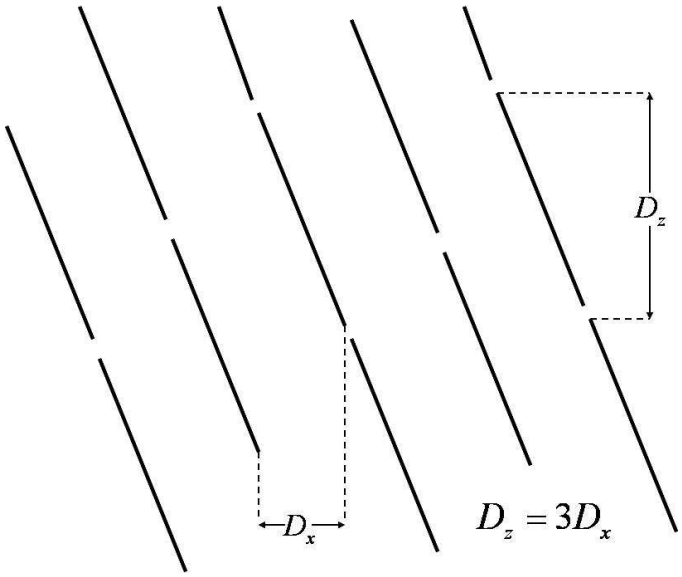

Figure 6.1: Two dimensional infinite array of short circuited dipoles

with respect to bandwidth, angle of incidence and grating lobes. In this research we have used a combination of the four legged loaded element and short circuited dipoles.

6.3.1 Short Circuited Dipoles

An array of short circuited dipoles was shown in Fig.1.3. They can also be arranged as shown in Fig.6.1 which is referred to as a gangbuster surface [47]. If the inter element spacing remains the same, the frequency of onset of grating lobes remains the same. The closer the elements, the higher is the frequency of the onset of grating lobes. However, the resonant frequency is dependent on the length of the dipole. The magnitude of the reflection coefficient for such surfaces is unity except for sharp nulls that occur only for oblique angles of incidence because of modal interaction [49]. An array of short circuited dipoles will respond to only one polarization. The reflection coefficient for the orthogonal polarization is much smaller, and the structure does not resonate. In order to respond to more than one polarization, an array of cross dipoles can be interlaced with the original array. This concept will be illustrated later, and it can be seen that this can also lead to a vector antenna structure.

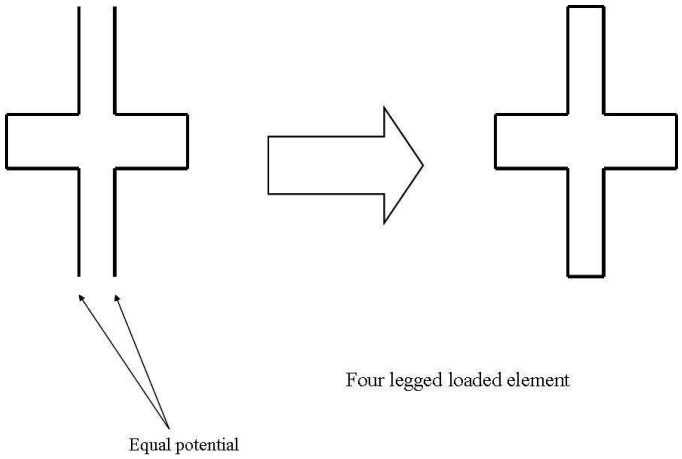

Figure 6.2: Formation of a four legged loop element from two dipoles

6.3.2 Four Legged Loaded Loop

The four legged loaded element is obtained by joining two loaded dipoles at their terminals [48](Fig.6.2). Some of the important properties of this structure are given here as outlined in [48]. One advantage of this structure is that it is equally capable of responding to horizontal as well as vertical polarizations. An array of elements is shown in Fig.6.3. All the loop structures have nulls for both polarizations when the lengths of loads are approximately $\lambda/4$. When this happens, the short circuit load appears at the dipole input as an open circuit effectively leading to no current flow. This happens for parallel as well as perpendicular polarizations as opposed to the modal interaction nulls in the center connected elements that occurs for only parallel polarization. This structure also provides opportunity for bandwidth control by changing the load impedance. This can be achieved by varying the distance between the arms of the loading element. A shorter distance decreases the bandwidth and vice versa. Above the first null, a second resonance occurs for both polarizations when the inductive self impedance of the dipole is canceled by the capacitive loading of the transmission line. However, for parallel polarization, and an oblique angle of incidence, an odd mode resonance occurs before the true second resonance, thereby moving the frequency of the true second resonance upwards.

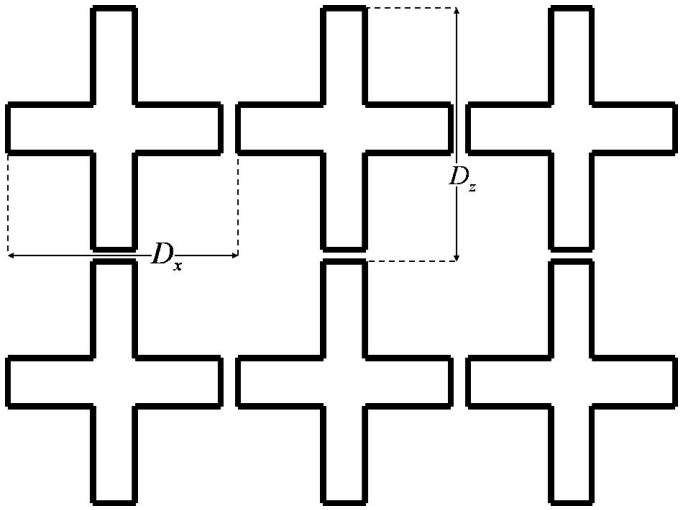

Figure 6.3: Two dimensional infinite array of four legged loop elements

6.4 Simulation Results

A number of structures were simulated using Ansoft's HFSS electromagnetic simulation package. HFSS is a finite element simulation program. The arrays of passive antennas were simulated as infinite arrays in two dimensions.

- Short circuited dipoles

  An infinite array of short circuited dipoles was the first structure to be simulated. The dipoles were designed to resonate at 8 GHz (which is the lower end of the X band commonly used for radar). Their length was determined by simulating active dipoles in ADS. The spacing between adjacent dipoles in the x and y directions were $D_x =$ 13.1 mm and $D_z = 22.2$ mm as shown in Fig.6.4. Fig.6.5 shows the reflection curve for parallel and perpendicular polarization and incidence angles of 0^o and 45^o. From the figure it can be seen that the surface is highly reflective when the incident E-field is polarized along the length of the dipole as in parallel polarization and is not reflective when the polarization is perpendicular. Also in parallel polarization, the curves are different for the different angles of incidence. Therefore the surface will have to be designed carefully to maintain the same resonance curve for the required angles of incidence.

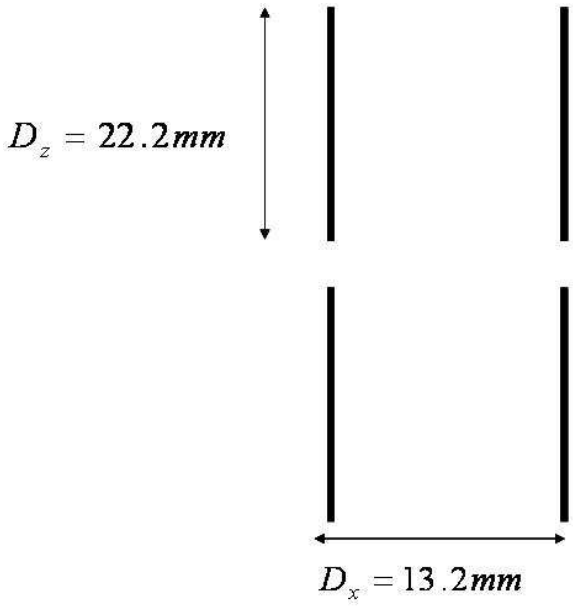

Figure 6.4: Two dimensional array of shorted dipole simulated in HFSS

- Four legged loaded element

  The four legged loaded element has a number of favorable properties such as a broad bandwidth, response to both polarizations as well as better stability of the reflection co-efficient with angles of incidence. The array of four legged elements is shown in Fig.6.6 and the simulation results are shown in Fig.6.7.

  From the figures it can be seen that the resonant frequency is stable for both polarizations and angles of incidence. However the bandwidth of the structure varies with the angle of incidence and grating lobes occur at higher frequencies for oblique angles of incidence. This structure can then be used in conjunction with dipoles to form novel structures.

- Combination element

  Consider a combination of the four legged loaded element and crossed dipoles. The crossed dipoles are connected at the center and are 11.1 mm long. This geometry is shown in Fig.6.8.

  The structure was simulated in HFSS for different polarizations and normal incidence. The loop is the same structure as shown in Fig.6.6 and the result for parallel polar-

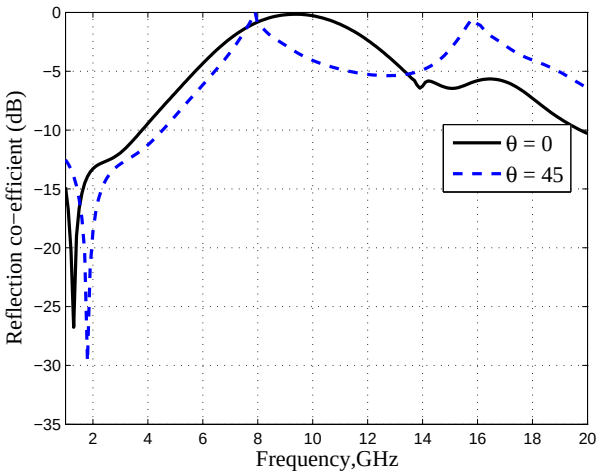

(a)

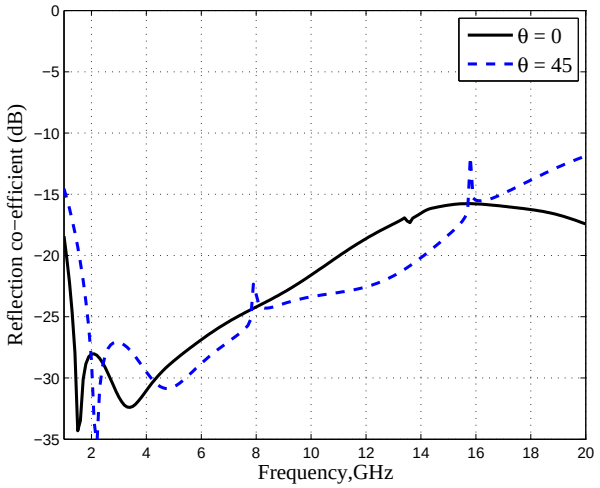

(b)

Figure 6.5: Simulated reflection curves of short circuited dipoles (a) Parallel polarization (b) Perpendicular polarization

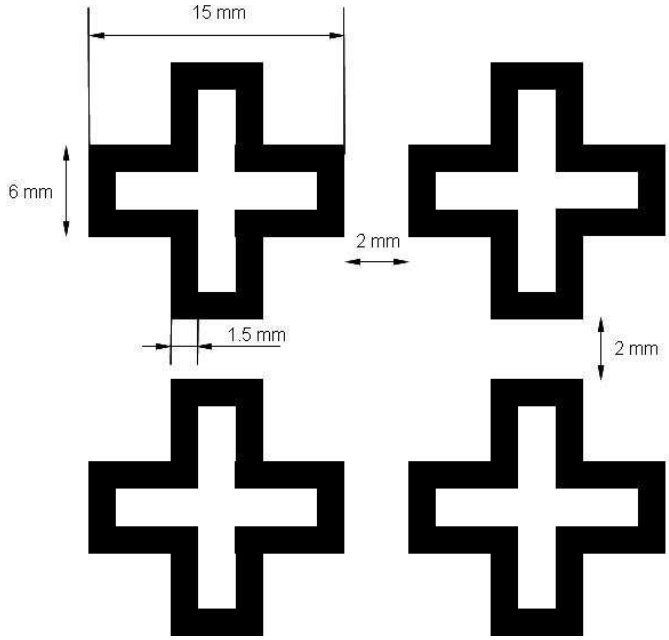

Figure 6.6: Two dimensional array of four legged loaded elements simulated in HFSS

ization is shown in Figure.6.9. The figure also shows the simulation results for the combination of cross dipoles. The dipole that is aligned in the direction of the electric field resonates while the other dipole produces no reflection. The dipole resonates when the incident electric field is along its length and produces a characteristic resonance at 13 GHz. Fig.6.10 shows the resonant curve of the combination element. It can be seen that there is a resonance around 7 GHz. This corresponds to the resonance of the loop element that is pulled slightly downward because of the increased capacitance on being loaded with the cross dipoles. The resonance at 13 GHz is the resonance because of the dipole. This resonance has been pulled downwards and has increased in bandwidth because of the capacitive loading. The final resonance occurs because the second resonance of the loop is pulled upwards because of insufficient capacitance to cancel out the inductance at the lower frequency. This cancelation then occurs at a slightly higher frequency. Thus we have three distinct resonances in the band 6 to 20 GHz.

The plots for perpendicular polarization are shown in Fig.6.11. The resonance curve of the loop remains the same because the structure is symmetric. Since the cross is

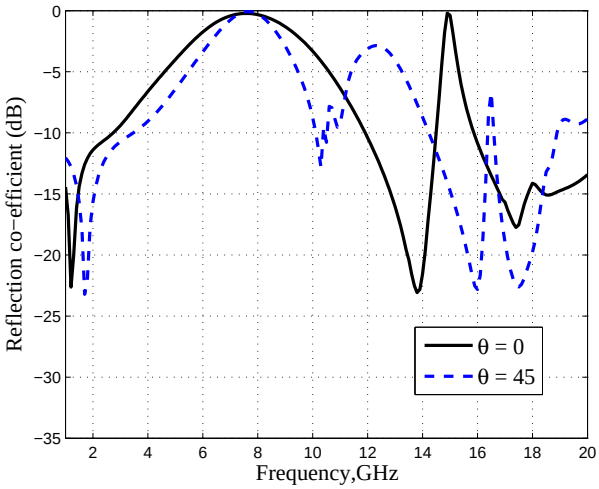

(a)

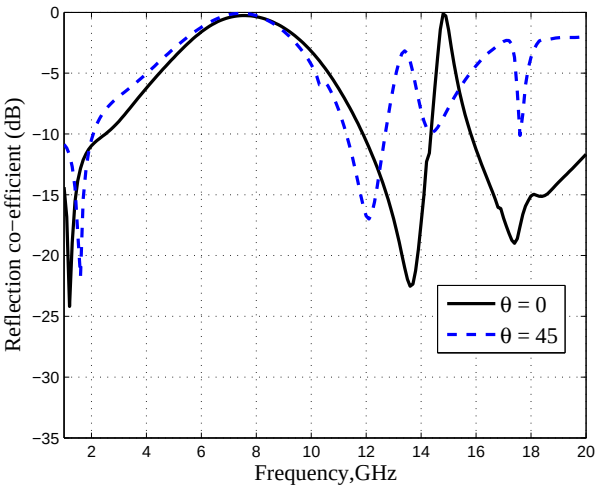

(b)

Figure 6.7: Simulated reflection curves of four legged loaded elements (a) Parallel polarization (b) Perpendicular polarization

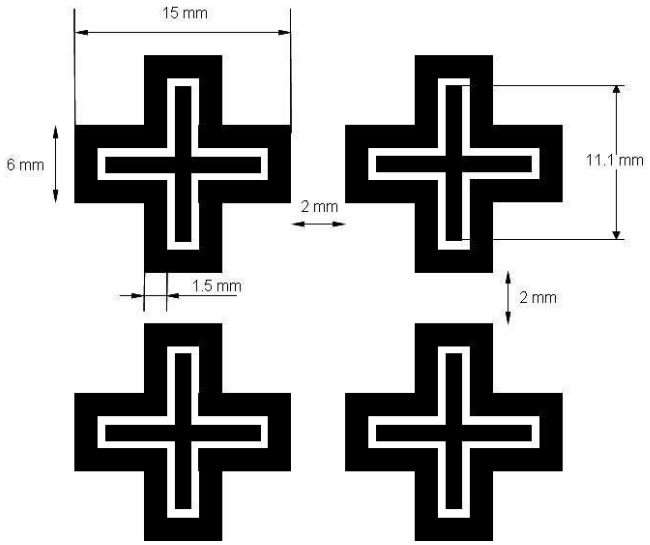

Figure 6.8: Two dimensional array of combination elements

also symmetric, we get identical responses for perpendicular polarization as well. The resonance curve for the combination structure is shown in Fig.6.12. It can be seen that the response is the same as for parallel polarization. In other words, we have the same reflection signature for two different orthogonal polarizations.

Since we have found that the combination structure responds to both the orthogonal polarizations, this potentially gives another degree of freedom by allowing us to vary the length of one of the dipoles producing an asymmetric cross. The length of the shorter dipole in this case is 9 mm and the structure is shown in Fig.6.13. The results for parallel polarization are exactly the same as in the previous case because the dipole aligned in the direction of parallel polarization is the same. Therefore only the results pertaining to perpendicular polarization are shown in Fig.6.14. The longer dipole does not resonate because it is orthogonal to the direction of polarization. The shorter dipole resonates naturally at around 15 GHz. The resonance curve for the combination element is shown in Fig.6.15. We can now see that for perpendicular polarization, we obtain a different resonance curve as compared to the parallel case (Fig.6.10). The second resonance occurs at around 13.5 GHz as opposed to 12.5 GHz in the parallel case. This gives us two different resonance curves in orthogonal directions giving a unique signature. The dipole lengths can be adjusted to different length to

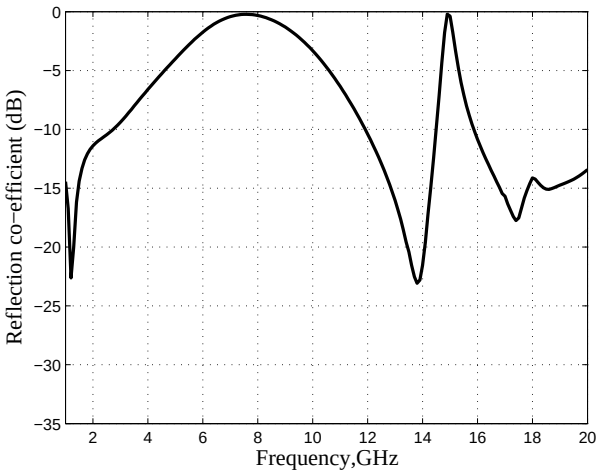

(a)

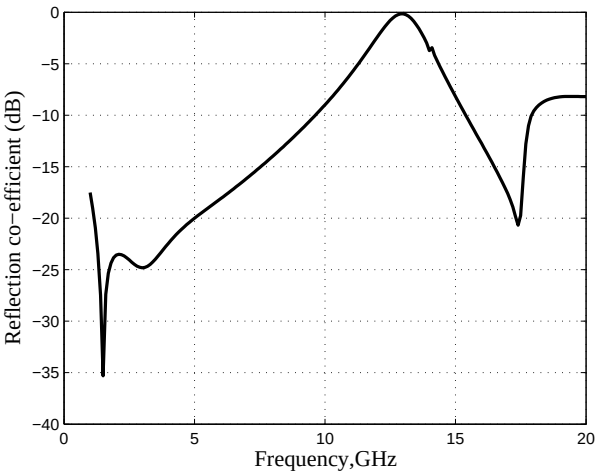

(b)

Figure 6.9: Simulated reflection curves of the loop and crossed dipoles in the combination element (Parallel polarization) (a) Loop (b) Cross

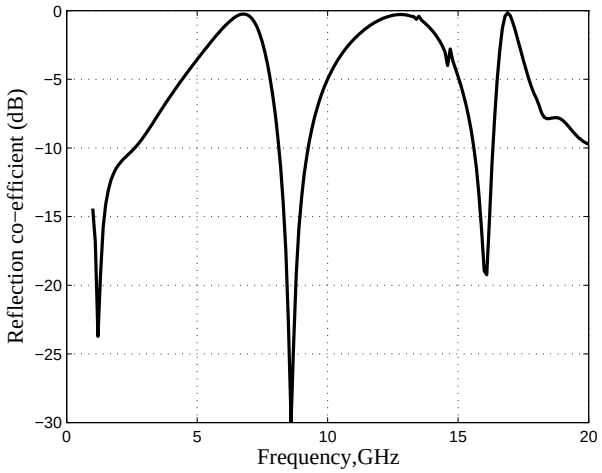

Figure 6.10: Reflection curve for the two dimensional array of combination elements (Parallel polarization)

give resonances at the frequency desired. However, it must be kept in mind that as the dipole length is made shorter, its resonant frequency increases and wavelength decreases. This implies that the inter-element spacing will be a greater fraction of the wavelength and this could lead to grating lobes. In case of an unloaded cross the bent mode exists and this could produce nulls for oblique angles of incidence. Since this structure provides different responses in two orthogonal directions, this principle can possibly be extended by using more dipoles oriented in different directions to obtain different signatures. An example of a multiply resonant FSS using tripoles and ternary shaped loops has been described in [50].

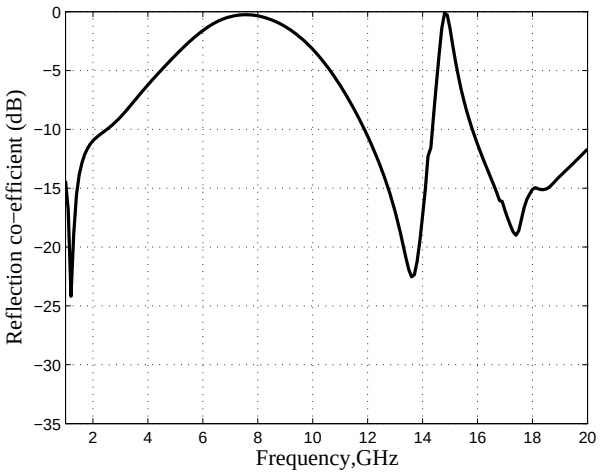

(a)

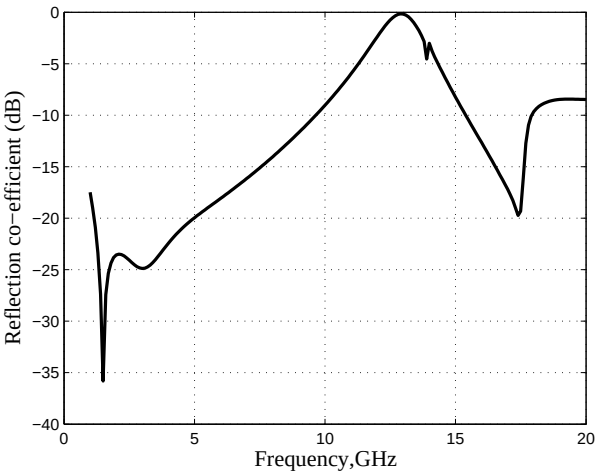

(b)

Figure 6.11: Simulated reflection curves of the loop and crossed dipoles in the combination element (Perpendicular polarization) (a) Loop (b) Cross

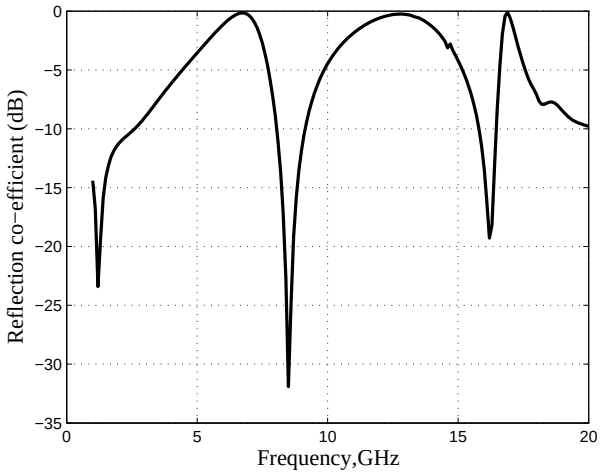

Figure 6.12: Reflection curve for the two dimensional array of combination elements (Perpendicular polarization)

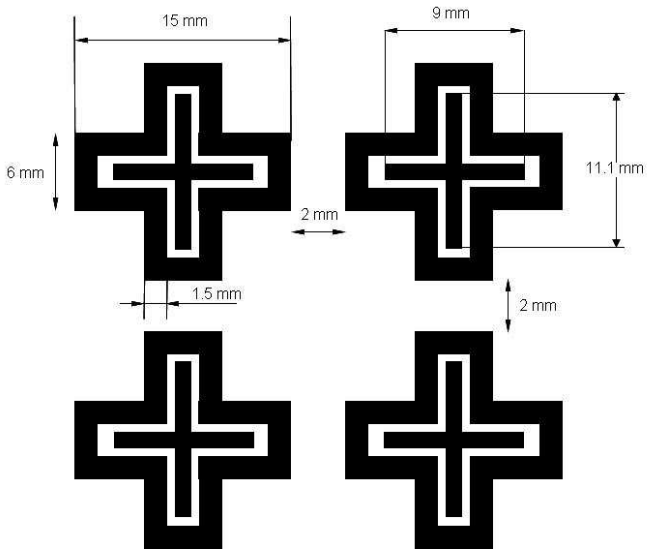

Figure 6.13: Geometry of the combination structure with unequal lengths of dipoles

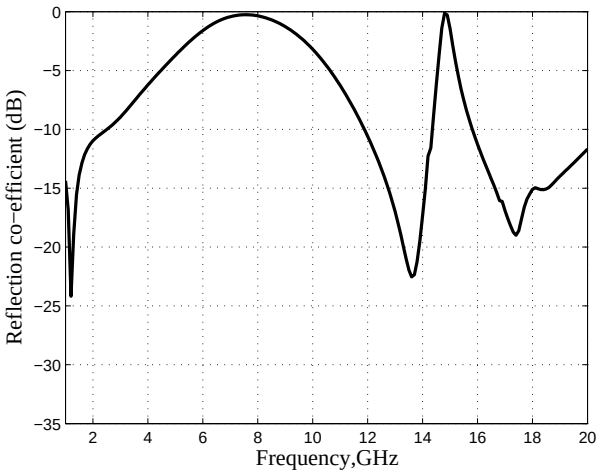

(a)

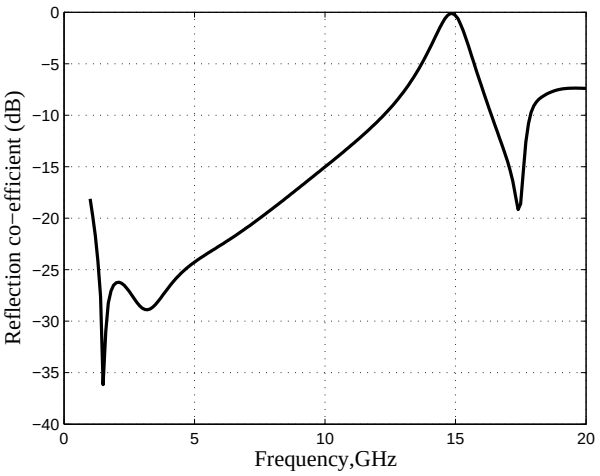

(b)

Figure 6.14: Simulated reflection curves of the loop and crossed dipoles with different lengths (Perpendicular polarization) (a) Loop (b) Cross

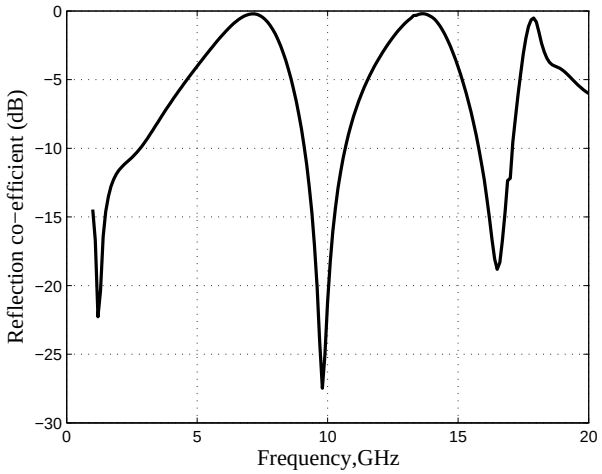

Figure 6.15: Reflection curve for the two dimensional array of combination elements with different length dipoles (Perpendicular polarization)

Chapter 7

Conclusions and Future Work

7.1 Summary of Contributions

This research presented novel solutions for vector antenna design applicable in ultra wide band systems and frequency selective surfaces. The important contributions are stated below.

7.1.1 Vector Antennas

A vector antenna responds to more than one polarization of the incident electromagnetic field. Co-located vector antennas were shown to provide an increase in wireless channel capacity as compared to a single antenna in the narrow band case [10]. In this research, this idea was extended to include ultra wide band antennas. A co-located ultra wide band vector antenna comprising a clover leaf loop antenna and two nearly orthogonal bowtie antennas was designed. The antennas operate over the frequency range from 3.6-8.5 GHz. The simulated radiation patterns of the antennas show that the individual antenna elements behave as a broadband loop and dipole respectively. The mutual coupling between the antennas was less than -15 dB for all cases. The antennas were tested for impulse radiation and were found to have a linear phase response. To evaluate the performance of these antennas in a real world scenario, the vector antenna was tested in the transmitter receiver configuration in the laboratory. Metal scatterers were placed in the far field of the antennas to simulate the wireless channel. The line of sight path was blocked. On evaluating the channel capacity it was found that this antenna system provided almost the

same capacity as that of a linear array with antennas separated by half a wavelength. The capacity obtained was also almost three time that obtained by using only a single antenna. This vector antenna therefore provides two additional degrees of freedom as compared to a single narrow band antenna, namely frequency and number of elements. Both these factors combine to produce a tremendous increase in channel capacity.

For applications that require less coupling between the antennas, another antenna configuration called the distributed vector antenna configuration was proposed. Distributed vector antennas for the narrow band case was designed and showed improvements in the direction of arrival estimation measurements [13]. A distributed vector antenna was also designed for the ultra wide band case with coupling less than -20 dB between the antenna elements. This produced similar results to the co-located vector antenna and occupied a smaller area.

7.1.2 Frequency Selective Surfaces

Frequency selective surfaces are spatial filters that are capable of producing unique signatures when an electromagnetic field is incident on them. This research investigated the use of vector antennas in frequency selective surfaces. It was shown that a structure comprising a four legged loaded antenna and cross dipoles can resonate at distinct frequencies producing a unique signature.

7.2 Future Work

7.2.1 Vector Antennas

Vector antenna miniaturization without distortion of the radiation pattern or impulse response can be investigated. Since there are six components of an electromagnetic field, the possibility of designing a six antenna system can be further investigated. A MIMO cube consisting of six antennas on the six faces of a cube has been proposed [51] and investigated [52]. A MIMO antenna containing 24 and 36 ports has been built and tested [53]. However, all these antennas have been proposed for narrow band systems. With the research reported in this thesis, the above configurations can be also extended to ultra wide band systems. However, antenna design will have to preserve certain essential characteristics required of an ultra wide band antenna, namely radiation pattern, impulse response

and impedance matching. Mutual coupling will also have to be taken into account because using more antennas in close proximity will lead to increased coupling.

The experiments in this work were carried out only with the antenna system in place. The channel response was measured by obtaining the S_{12} parameter. Although this provides the bounds that capacity can achieve, it does not take into account the effect of other parts of a communication system. Any communication system consists of transmitter and receiver circuitry and also has its own modulation schemes and coding schemes. Some modulation schemes used in ultra wide band systems were described in Chapter 1. It would be very useful to determine the actual capacity obtained when the antennas investigated in this work are used in a complete communication system to send and receive information in the form of bits. This will require that each antenna is connected to an RF chain which in turn is connected to a source of information. The design of RF chains, the corresponding signal processing algorithms, choosing the modulation scheme and antenna selection etc. are very important problems to be solved when the communication system is considered in its entirety. Optimization of each component of the system as well as overall optimization of the system will have to be carried out to obtain maximum possible capacity. This is a very interesting avenue of research that can be pursued and has immediate practical applications.

These vector antennas can also be investigated for active microwave imaging for tumor detection in breast cancer.This detection is based on the contrast in dielectric properties between these tissues, which is often a factor of 2-7 at microwave frequencies which results in significant scattering from the malignancy. Since ultra wide band signaling uses very narrow impulses greater resolution can be obtained in detection.

The ultra wide band distributed vector antenna was shown to provide an increase in capacity similar to the co-located vector antenna. This antenna can be further investigated for direction of arrival estimation (DOA). Linear arrays that are used now in DOA applications require a large number of antennas, and perform poorly in the presence of multipath components. In order to overcome these difficulties, a vector antenna can be used. A vector antenna can perform better under fading conditions and also reduce ambiguity in DOA estimation. Since improvements with distributed vector antenna have been reported in the narrow band case [13], further improvements can be expected using ultra wide band antennas.

7.2.2 Frequency Selective Surfaces

It has been shown that by using a combination of simple elements of frequency selective surfaces, a multiple resonance structure is obtained that has a significant reflection normal to the surface. This idea can be used to further design surfaces that resonate at particular frequencies to provide unique signatures. The surface can also be modeled as an equivalent circuit composed of lumped elements that resonates at the same frequencies. This circuit can offer additional insights on the design of the frequency selective surface (FSS) and can be used to modify the resonant properties as required. As pointed out in [48], the unloaded cross has instability with respect to angle of incidence and polarization. We have shown that the multiply resonant structure works for normal incidence. Specifically, a null occurs between two resonances of the cross because of the excitation of a crooked or bent mode. This problem can be solved by increasing the edge capacitance of the cross using capacitive loading. This can be done by a staggered arrangement of the crosses as proposed in [54] or using a Jerusalem cross shown earlier. In our case, capacitive loading can be increased by using a Jerusalem cross inside the outer loop or using a staggered arrangement as shown in Fig.7.1.

Some applications of these FSS's include the blocking of signals from wireless communication networks for security purposes. For example, consider a wireless network being used inside a room in a building. If it is desired that the data exchanged over this network remain private, secure and confidential, then the walls of the room can be covered with a frequency selective surface that reflects back signals at frequencies used in the wireless network. This will ensure that no signal 'leaks' outside the room and thereby ensuring security of the network from a physical layer standpoint. Some research in this area has been described in [50],[55].

The frequency selective surfaces described in this research have been studied using simulations only. These surfaces have to be tested practically. This will require the design of a calibrated experimental setup which will involve solving a number of practical problems.

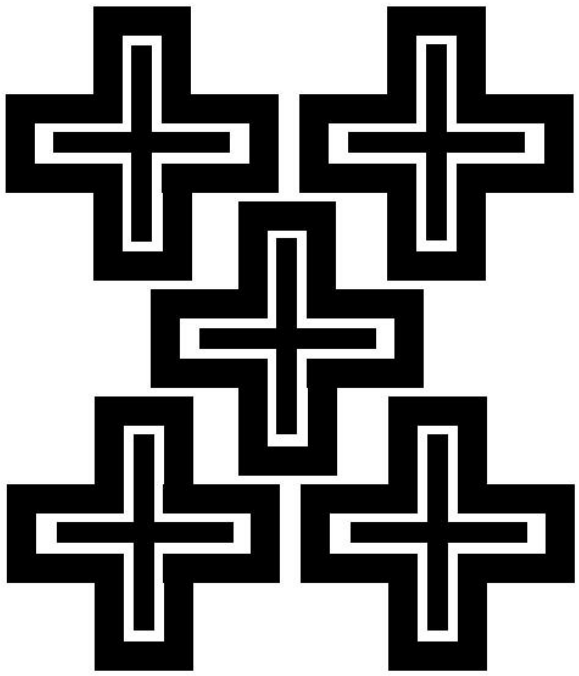

(*a*)

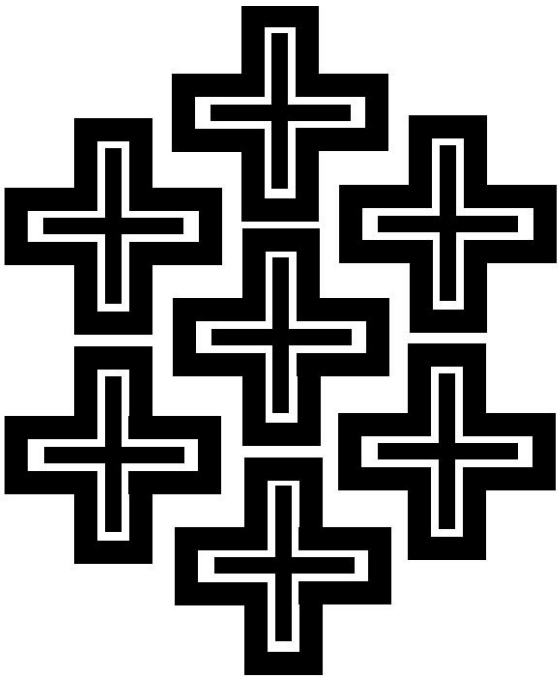

(*b*)

Figure 7.1: Two methods of producing staggering

Bibliography

[1] P. H. Smith. "Cloverleaf " Antenna for F.M. Broadcasting. *Proceedings of the IRE*, pages 1556–1563, Dec. 1947.

[2] M.G.Di Benedetto, T.Kaiser, A.F.Molisch, I.Oppermann, C.Politano, and D.Porcino. *UWB Communication Systems: A Comprehensive Overview*, volume 5 of *EUARAISP Book Series on Signal Processing and Communcations*. Hindawi Publishing Corporation, 2006.

[3] M.Ghavami, L.B.Michael, and R.Kohno. *Ultra wideband signals and systems in communication engineering*. John Wiley and Sons, 2004.

[4] H.Arslan, Z.N.Chen, and M.G.Di Benedetto. *Ultra Wideband Wireless Communication*. John Wiley and Sons, 2006.

[5] Federal Communications Commission (2002b). FCC First Report and Order in the matter of revision of part 15 of the commission's rules regarding ultra wideband transmission systems. *ET-Docket*, pages 98–153, April 2002.

[6] G. J. Foschini and M.J.Gans. On limits of wireless communications in a fading environment when using multiple antennas. *Wireless Personal Communications*, 6:311–335, Jun. 1998.

[7] E. Telatar. Capacity of multi-antenna Gaussian channels. *European Transactions on Telecommunications*, 10(6):585–595, Jul. 1999.

[8] B.A.Cetiner, E.Akay, E.Sengul, and E.Ayanoglu. A MIMO System With Multifunctional Reconfigurable Antennas. *IEEE Antennas Wireless Propagation Letters*, 5:463–466, 2006.

[9] M. R. Andrews, P. P. Mitra, and R. deCarvalho. Tripling the Capacity of Wireless Communications Using Electromagnetic Polarization. *Nature*, 409:316–318, Jan. 2001.

[10] A. S. Konanur, K. Gosalia, S. H. Krishnamurthy, B. Hughes, and G. Lazzi. Increasing Wireless Channel Capacity Through MIMO Systems Employing Co-Located Antennas. *IEEE Transactions on Microwave Theory and Techniques*, 53(6):1837–1844, Jun. 2005.

[11] A.K.Y.Lai, A.L.Sinopoli, and W.D.Burnside. A Novel Antenna for Ultra-Wide-Band Applications. *IEEE Transactions on Antennas and Propagation*, 40(7):755–760, Jul. 1992.

[12] E.Fishler, A.Haimovich, R.Blum, D.Chizhik, L.Cimini, and R.Valenzuela. MIMO Radar: An Idea Who's Time Has Come. In *Proceedings of the IEEE Radar Conference*, pages 71–78, 2004.

[13] L.Lo Monte, B.Elnour, A.Rajagopalan, G.Gupta, D.Erricolo, and G.Lazzi. Circularly and Linearly Distributed Narrowband Vector Antennas for Direction of Arrival Applications. In *URSI North American Radio Science Meeting*, Ottawa,Canada, July 2007.

[14] X. Li, S. Davis, S.Hagness, D. van der Weide, and B.Veen. Microwave imaging via space-time beamforming: experimental investigation of tumor detection in multilayer breast phantoms. *IEEE Transactions on Microwave Theory and Techniques*, 52(8):1856–1865, Aug. 2004.

[15] S.Hagness, A.Taflove, and J.Bridges. Three-dimensional fdtd analysis of a pulsed microwave confocal system for breast cancer detection: design of an antenna-array element. *IEEE Transactions on Antennas and Propagation*, 47(5):783–791, May. 1999.

[16] E. Fear and M. Stuchly. Microwave breast tumor detection: antenna design and characterization. In *IEEE Antennas and Propagation Society International Symposium*, volume 2, pages 1076–1079, July 2000.

[17] C.A. Balanis. *Antenna Theory: Analysis and Design.* John Wiley and Sons, 2002.

[18] S.A.Schelkunoff and H.T.Friis. *Antennas: Theory and Practice*, pages 504–508. John Wiley and Sons, 1952.

[19] H.Schantz. *The Art and Science of Ultrawideband Antennas*, pages 176–177 and 238–240. Artech House, 2005.

[20] H.Schantz. UWB Magnetic Antennas. In *IEEE International Symposium on Antennas and Propagation*, pages 604–607, Columbus, OH, USA, June. 2003.

[21] N.Behdad and K.Sarabandi. A Compact Antenna for Ultrawide-Band Applications. *IEEE Transactions on Antennas and Propagation*, 53(7):2185–2192, Jul. 2005.

[22] H.Nakano, M.Fukasawa, and J.Yamauchi. Multi-Frequency and Wide-Band VSWR Characteristics of Loop Antennas. In *IEEE International Symposium on Antennas and Propagation*, pages 1524–1527, July. 2000.

[23] C.E.Baum and E.G.Farr. Impulse Radiating Antennas. In H.L.Bertoni, L.Carin, and L.B.Felsen, editors, *Ultra-Wideband, Short-Pulse Electromagnetics*. New York:Plenum, 1993.

[24] H.Schantz. UWB Planar Bulbous Dipole Antennas. In *IEEE International Symposium on Antennas and Propagation*, pages 475–478, Washington D.C., USA, July. 2005.

[25] J.Powell and A.Chandrakasan. Differential and Single Ended Elliptical Antennas for 3.1-10.6 GHz Ultra Wideband Communication. In *IEEE International Symposium on Antennas and Propagation*, pages 2935–2938, June 2004.

[26] G.Lu, S.von der Mark, I.Korisch, L.J.Greenstein, and P.Spasojevic. Diamond and Rounded Diamond Antennas for Ultrawide-Band Communications. *IEEE Antennas and Wireless Propagation Letters*, 3:249–252, 2004.

[27] N.Fortino, G.Kossivas, J.Y.Dauvignac, and R.Staraj. Novel Antennas for Ultra-WideBand Communications. *Microwave and Optical Technology Letters*, 41(3):166–169, May 2004.

[28] R.C.Johnson and H.Jasik, editors. *Antenna Engineering Handbook*. McGraw-Hill,New York, 1984.

[29] H.Ghannoum, S.Bories, C.Roblin, and A.Sibille. Biconical Antennas for intrinsic characterization of the UWB Channel. In *IEEE International Workshop on Antenna Technology: Small Antennas and Novel Metamaterials*, pages 101–104, Washington D.C., USA, March 2005.

[30] G.H.Brown and O.M.Woodward. Experimentally Determined Radiation Characteristics of Conical and Triangular Antennas. *RCA Review.*, 13(4), December 1952.

[31] X.H.Wu and Z.N.Chen. Comparison of Planar Dipoles in UWB Applications. *IEEE Transactions on Antennas and Propagation*, 53(6):1973–1983, Jun. 2005.

[32] A.A.Lestari, A.G.Yarovoy, and L.P.Ligthart. RC-Loaded Bow-Tie Antenna for Improved Pulse Radiation. *IEEE Trans. Antennas Propagat.*, 52(10):2555–2563, Oct. 2004.

[33] K. Kiminami, A.Hirata, and T.Shiozawa. Double-Sided Printed Bow-Tie Antenna for UWB Communications. *IEEE Antennas and Wireless Propagation Letters*, 3:152–153, 2004.

[34] A. A. Eldek, A. Z. Elsherbeni, and C. E. Smith. Wide-Band Modified Printed Bow-Tie Antenna With Single and Dual Polarization for C and X-Band Applications. *IEEE Transactions on Antennas and Propagation*, 53(9):3067–3072, Sep. 2005.

[35] T.Svantesson and A.Ranheim. Mutual Coupling Effects on the Capacity of Multielement Antenna Systems. In *IEEE International Conference on Acoustics Speech and Signal Processing*, pages 2485–2488, June 2001.

[36] A.Rajagopalan, G.Gupta, A.Konanur, B.L.Hughes, and G.Lazzi. Increasing Channel Capacity of an Ultrawideband MIMO system using Vector Antennas. *IEEE Transactions on Antennas and Propagation*, 55(10):2880–2887, Oct. 2007.

[37] R.Janaswamy. Effect of Element Mutual Coupling on the Capacity of Fixed Length Linear Arrays. *IEEE Antennas and Wireless Propagation Letters*, 1:157–162, 2002.

[38] I.Oppermann, M.Hamalainen, and J.Iinatti. *UWB Theory and Applications.* John Wiley and Sons, 2004.

[39] I.Oppermann, M.Hamalainen, and J.Iinatti. *UWB Theory and Applications*, pages 20–21. John Wiley and Sons, 2004.

[40] I.Oppermann, M.Hamalainen, and J.Iinatti. *UWB Theory and Applications*, pages 10–11. John Wiley and Sons, 2004.

[41] A.S.Jazi, A.M.Attiya, and S.Riad. Channel Measurement and Simulation. In J.H.Reed, editor, *An Introduction to Ultra Wide Band Communication Systems*. Prentice Hall, PTR, Upper Saddle River, NJ, 2005.

[42] C.C.Chong and S.K.Yong. A Generic Stastical-Based UWB Channel Model for High-Rise Apartments. *IEEE Transactions on Antennas and Propagation*, 53(8):2389–2399, Aug. 2005.

[43] K.Sarabandi, N.Behdad, A.Nashashibi, M.Casciato, L.Pierce, and F.Wang. A Measurement System for Ultrawide-Band Communication Channel Characterization. *IEEE Transactions on Antennas and Propagation*, 53(7):2146–2155, Jul. 2005.

[44] A.S. Konanur. *An Investigation on Vector Antennas*. PhD thesis, North Carolina State University, Raleigh, NC, 2006.

[45] M.C.Mtumbuka and D. J. Edwards. Investigation of Tri-polarised MIMO Technique. *Electronics Letters*, 41(3):137–138, Feb. 2005.

[46] M.C. Mtumbuka, W.Q.Malik, C. J. Stevens, and D.J.Edwards. A Tri-Polarized Ultra-Wideband MIMO System. In *Proc. IEEE Sarnoff Symposium on Advances in Wired and Wireless Communications*, pages 98–101, Princeton, NJ, USA, Apr. 2005.

[47] B.A.Munk. *Frequency Selective Surfaces Theory and Design*. John Wiley and Sons, 2000.

[48] B.A.Munk. *Frequency Selective Surfaces Theory and Design*, pages 26–55. John Wiley and Sons, 2000.

[49] B.A.Munk. *Frequency Selective Surfaces Theory and Design*, pages 30–32. John Wiley and Sons, 2000.

[50] D.H.Kim and J.I.Choi. Frequency Selective Surface for the blocking of multiple frequency bands. In *IEEE International Symposium on Antennas and Propagation*, pages 4195–4197, July 2006.

[51] B.N.Getu and J.B.Andersen. The MIMO cube: A Compact MIMO Antenna. *IEEE Transactions on Wireless Communications*, 4:1136–1141, May 2005.

[52] B.N.Getu and R.Janaswamy. The Effect of Mutual Coupling on the Capacity of the MIMO Cube. *IEEE Antennas and Wirless Propagation Letters*, 4:240–244, 2005.

[53] C.Y.Chiu, J.B.Yan, and R.D.Murch. 24-Port and 36-Port Antenna Cubes Suitable for MIMO Wireless Communications. *IEEE Transactions on Antennas and Propagation*, 56(4):1170–1176, April 2008.

[54] T.W. Kornbau. *Analysis of periodic Arrays of Rotated Linear Dipoles, Rotated Crossed Dipoles, and of Biplanar Dipole Arrays in Dielectric*. PhD thesis, Ohio State University, Columbus,OH, 1984.

[55] G.I.Kiani, A.R.Weily, and K.P.Esselle. Frequency Selective Surface Absorber Using Resisitve Cross-Dipoles. In *IEEE International Symposium on Antennas and Propagation*, pages 4199–4202, July 2006.